FILE COPY
NO. 4

CASE FILE
COPY

NACA TN No. 1649

NATIONAL ADVISORY COMMITTEE FOR AERONAUTICS

TECHNICAL NOTE

No. 1649

INVESTIGATION OF A $\frac{1}{7}$-SCALE POWERED MODEL OF A TWIN-BOOM AIRPLANE AND A COMPARISON OF ITS STABILITY, CONTROL, AND PERFORMANCE WITH THOSE OF A SIMILAR ALL-WING AIRPLANE

By Gerald W. Brewer and Ralph W. May, Jr.

Langley Aeronautical Laboratory
Langley Field, Va.

THIS DOCUMENT ON LOAN FROM THE FILES OF

NATIONAL ADVISORY COMMITTEE FOR AERONAUTICS
LANGLEY AERONAUTICAL LABORATORY
LANGLEY FIELD, HAMPTON, VIRGINIA

RETURN TO THE ABOVE ADDRESS.

REQUESTS FOR PUBLICATIONS SHOULD BE ADDRESSED AS FOLLOWS:

NATIONAL ADVISORY COMMITTEE FOR AERONAUTICS
1724 F STREET, N.W.,
WASHINGTON 25, D.C.

Washington
October 1948

NATIONAL ADVISORY COMMITTEE FOR AERONAUTICS

TECHNICAL NOTE NO. 1649

INVESTIGATION OF A $\frac{1}{7}$-SCALE POWERED MODEL OF A TWIN-BOOM AIRPLANE AND A COMPARISON OF ITS STABILITY, CONTROL, AND PERFORMANCE WITH THOSE OF A SIMILAR ALL-WING AIRPLANE

By Gerald W. Brewer and Ralph W. May, Jr.

SUMMARY

An investigation of a $\frac{1}{7}$- scale powered model of a twin-boom airplane was conducted in order to obtain a comparison of its stability, control, and performance characteristics with those of an all-wing-airplane design of the same over-all proportions. These models represent very large airplanes having a gross weight of nearly 90 tons, a wing span of 290 feet, and an aspect ratio of 10.6. The test results of the all-wing design have been previously reported. The test results of the twin-boom model are presented in this paper together with a summary comparison of the characteristics of the two types of airplane.

At the design center-of-gravity location of 0.23 mean aerodynamic chord the twin-boom airplane had about a 3-percent static margin in the high-speed range with rated power and about a 5-percent static margin at low speed with propellers windmilling and flap deflected 40°. In comparison, the all-wing airplane had a somewhat larger static margin for rated-power operation but much less static longitudinal stability at low speeds with propellers windmilling.

The twin-boom airplane possessed generally stable or neutrally stable variations of trim elevator deflection with airspeed for all conditions except for rated power with the flap deflected. The twin-boom airplane had less stable trim elevator-deflection variations with airspeed than the all-wing airplane because of the combination of the lower degree of static longitudinal stability and increased elevator effectiveness. In general, the twin-boom airplane had neutrally stable trim elevator hinge-moment variations with airspeed as compared with the more stable variations for the all-wing airplane. The elevator effectiveness of the twin-boom airplane was nearly twice that for the all-wing airplane.

Each airplane had a low degree of static directional stability and also had a very low effective dihedral angle. The side force developed by the twin-boom airplane in yaw was very low and was approximately one-half that of the all-wing airplane.

The power of the rudders to trim the airplanes directionally was low, such that in the landing conditions with the propellers windmilling the twin-boom airplane could be trimmed to only 8.5° yaw and the all-wing airplane to only slightly greater angles.

The maximum trimmed lift coefficients of 1.31 for the twin-boom airplane and 1.03 for the all-wing airplane gave stalling speeds at sea level of 82 and 92 miles per hour, respectively. The investigation indicated that both airplanes will have essentially the same performance in range and rate of climb, but the reduction in drag for the twin-boom airplane at high lift coefficients represented increased performance over the all-wing airplane in take-off.

INTRODUCTION

A previous investigation of a $\frac{1}{7}$-scale powered model of an all-wing airplane in the Langley full-scale tunnel indicated that the all-wing airplane would probably meet the flying-qualities requirements for large airplanes provided that the low-speed characteristics were improved. In order to evaluate the performance characteristics of this particular all-wing design as compared with those of an airplane of more conventional design, tests were made of a twin-boom model having the same scale and power as the all-wing configuration. These models represent very large airplanes of about 90-ton gross weight with a 290-foot wing span and with a total of 6800 rated brake horsepower.

This paper presents the aerodynamic characteristics, the control-surface effectiveness, and a brief analysis of the static stability and control characteristics of the twin-boom airplane as well as some general comparisons between the test results of the twin-boom airplane and the previously obtained test results of the all-wing airplane. From the determination of the lift and drag characteristics of the two models, performance comparisons related to stalling speed, take-off run, range, and rate of climb are also presented.

In this present investigation the effects of elevator, rudder, and aileron deflection on the model forces and moments and on elevator and rudder hinge moments were obtained with angle of attack, angle of yaw, flap deflection, and power condition being the important variable parameters. A yaw range of -10° to 15° was investigated. For tests

with the flap deflected, a maximum deflection of 40° was used. The elevator tests were run for several constant thrust coefficients at a given angle of attack; the aileron tests, with propellers windmilling; and the rudder tests, with propellers windmilling, rated power, and asymmetric power. Additional tests included the determination of the effect of stabilizer and flap setting on the model forces and moments and also included the determination of the stall progression over the wing.

COEFFICIENTS AND SYMBOLS

The test data are presented as standard NACA coefficients of forces and moments. All data are referred to the stability axes, which are defined as a system of axes having the origin at the airplane center of gravity. The Z-axis is in the plane of symmetry and perpendicular to the relative wind, the X-axis is in the plane of symmetry and perpendicular to the Z-axis, and the Y-axis is perpendicular to the plane of symmetry. The positive directions of forces and moments and control-surface deflections are shown in figure 1. Values given for areas and lengths in this section relate to the model dimensions.

C_L lift coefficient (Lift/qS)

C_X longitudinal-force coefficient (X/qS)

C_Y lateral-force coefficient (Y/qS)

C_m pitching-moment coefficient (M/qSc')

C_n yawing-moment coefficient (N/qSb)

C_l rolling-moment coefficient (L/qSb)

C_{h_e} elevator hinge-moment coefficient $\left(H_e/qb_e\bar{c}_e^{\,2}\right)$

C_{h_r} rudder hinge-moment coefficient $\left(H_r/qb_r\bar{c}_r^{\,2}\right)$

$C_{l_\psi} = \dfrac{\partial C_l}{\partial \psi}$

$C_{n_\psi} = \dfrac{\partial C_n}{\partial \psi}$

$C_{Y_\psi} = \frac{\partial C_Y}{\partial \psi}$

$C_{h_\alpha} = \frac{\partial C_h}{\partial \alpha}$

$C_{h_\delta} = \frac{\partial C_h}{\partial \delta}$

$C_{n_\delta} = \frac{\partial C_n}{\partial \delta}$

$C_{Y_\delta} = \frac{\partial C_Y}{\partial \delta}$

Q_c'	torque coefficient $\left(\frac{T_c'}{\eta} \frac{V}{nD} \frac{1}{2\pi} \frac{S}{2D^2}\right)$
T_c'	effective-thrust coefficient (T_e/qS)
V/nD	propeller advance-diameter ratio
X,Y,Z	forces along axes, pounds
L,M,N	moments about axes, foot-pounds
q	free-stream dynamic pressure, pounds per square foot $(\rho V^2/2)$
S	wing area (161.6 sq ft)
b_e	elevator span (6.40 ft)
b_r	rudder span (3.06 ft)
c'	mean aerodynamic chord (3.9 ft)
$\bar{c}_e$	root-mean-square elevator chord (0.644 ft)
$\bar{c}_r$	root-mean-square rudder chord (0.454 ft)
b	wing span (41.4 ft)
H	hinge moment, foot-pounds
W	airplane weight, pounds

T_e effective thrust of all propellers $(X - X_{\text{propeller removed}})$

V free-stream velocity, feet per second unless indicated otherwise

n propeller speed, revolutions per second

D propeller diameter (2.167 ft)

ρ mass density of air, slugs per cubic foot

α angle of attack of thrust axis relative to free-stream direction, degrees

ψ angle of yaw, degrees

δ control-surface deflection, degrees

$\beta_{0.75R}$ propeller-blade angle at 0.75 radius, degrees

n_p neutral-point location, percent mean aerodynamic chord (center-of-gravity location for neutral stability in trimmed flight)

i_t horizontal-stabilizer setting relative to thrust line, degrees

η propeller efficiency, percent

Subscripts:

e elevator

r rudder

a aileron

f flap

max maximum

DESCRIPTION OF AIRPLANE AND MODEL

Airplane

The full-scale twin-boom airplane corresponding to the model used in this investigation would have a design gross weight of 177,500 pounds,

a wing area of 7920 square feet, and a span of 290 feet. The power plants would consist of four Pratt & Whitney R-2800-C engines in tractor installation driving 15-foot-diameter four-blade propellers. The proposed all-wing airplane, to which comparison is made in this paper, would have the same wing except for an upward instead of a downward reflex at the trailing edge and four vertical surfaces located at the trailing edge of the center section. The important physical and dimensional characteristics of both airplanes, based on the design of the $\frac{1}{7}$-scale models, are presented in table I.

Model

As a matter of expedience the $\frac{1}{7}$-scale model of the all-wing airplane, described in reference 1, was utilized in the present investigation by inverting the wing, removing the four vertical tail surfaces, and installing a twin-boom tail. The 0.13c' plain flap for the twin-boom airplane was located at the trailing edge of the center section between the tail booms and replaced the original elevator of the all-wing design. The small amount of negative dihedral that resulted from inverting the original wing to obtain some effective camber would be expected to reduce the dihedral effect somewhat but would not be expected to introduce any first-order effects on the other aerodynamic characteristics. It was possible to utilize the advantage of increased effective camber of the inverted original wing and to compensate for the resulting change in trim by the addition of the horizontal tail.

Photographs of the twin-boom model tested in the Langley full-scale tunnel are shown as figure 2, and three-view drawings of the twin-boom and all-wing models with essential dimensions given are shown as figure 3. The wing, of aspect ratio 10.6, consisted of two highly tapered outer panels attached to a constant-chord center section. The airfoil sections were modified NACA 6-series type with the rear 15 percent of the trailing edge reflexed downward along the entire span.

The solid-mahogany control surfaces included a constant-percent-chord aileron on the right outboard panel, a vertical tail surface on the end of each boom, and a constant-chord horizontal tail surface placed between the vertical fins. The boom angle of 13° relative to the thrust line was determined from considerations of the requirements for landing. The blunt-nose plain-flap-type control surfaces were not sealed and were not equipped with tabs. The control linkages projected above the skin surface on the model but were covered with streamline fairings to minimize the drag. (See figs. 2(b) and 2(c).)

The model was powered by four 56-horsepower, three-phase induction motors located in the center section of the wing. Power was transmitted to the four-blade propellers of right rotation by direct drive through extension shafts. The model was not equipped with a landing gear and the nacelles had neither internal ducting nor cowl flaps.

METHODS AND TESTS

The $\frac{1}{7}$-scale model of the twin-boom airplane was mounted on two main support struts and a forward strut which, by varying the length, provided a means of changing the angle of attack. The Langley full-scale tunnel and balance system used for the tests are described in reference 2.

In order to simulate the flight thrust-lift relationship in the wind tunnel, a thrust calibration of the model propellers was made at a tunnel speed of approximately 54 miles per hour. The effective-thrust coefficient T_c' for the model propellers was determined from the difference between the propellers-operating and the propellers-removed longitudinal-force coefficients obtained with the model in the attitude for zero lift with all controls neutral. The model propeller blades were set at 17° at the 0.75 radius for these tests; this setting permitted a close approximation of the flight torque-lift relationship and an exact simulation of the flight thrust-lift relationship. The calculated flight thrust-lift coefficient curves for single-engine operation at constant rated power at sea level are shown in figure 4 together with the torque-lift coefficient curves for flight and for the model with propellers set at 17°. The curve of T_c' plotted against C_L for one propeller windmilling is also included.

All data presented in the paper have been corrected for wind-tunnel blocking and jet-boundary effects by the methods of reference 3 and for the drag tares of the support system. Pitching moments have been based on the mean aerodynamic chord.

The tests of the $\frac{1}{7}$-scale model of the twin-boom airplane consisted mainly of elevator-effectiveness, rudder-effectiveness, and aileron-effectiveness tests at zero yaw and rudder tests with the model yawed to angles of approximately $\pm 5^\circ$, $\pm 10^\circ$, and 15° with the flap both retracted and deflected 40°. Elevator and rudder hinge moments were measured at zero yaw. In addition, tests were made to determine the flap and horizontal-stabilizer effectiveness. The stalling characteristics of the wing were obtained for an angle-of-attack range through the stall with the propellers windmilling.

The propellers-operating elevator tests were made with the flap both retracted and deflected 40° by the constant-thrust test method in which several thrust coefficients were held constant through the range of elevator deflections tested at a given angle of attack. In the rudder tests at all yaw angles, the propellers-windmilling power condition was run with the flap deflected 40°; the rated and asymmetric power conditions were run with the flap retracted. In addition, at zero yaw the propellers-windmilling condition was run with the flap retracted and the rated-power condition with the flap deflected 40°. Tests with asymmetric power consisted of three-engine operation at rated power and with the left outboard propeller windmilling. The constant-rated-power thrust-lift coefficient curve of figure 4 that was employed for all the tests at zero yaw was also used for the rudder tests with the model yawed.

All tests of the present investigation were made at a tunnel airspeed of about 54 miles per hour corresponding, at standard conditions, to a Mach number of 0.07 and a Reynolds number of approximately 1.98×10^6 based on the mean aerodynamic chord.

RESULTS AND DISCUSSION

Presentation of Results

The results of the present investigation are given in the summary curves of figures 5 to 17 which are derived from the original test data presented in figures 18 to 35. The original data are presented for the most part as variations of force, moment, and hinge-moment coefficients with control-surface deflection for a range of angle of attack at a given power condition, flap position, and angle of yaw. The greater emphasis in the discussion of results is placed on the summary curves, which include the longitudinal and directional stability and control-surface characteristics, and on the performance estimates for the airplanes. All moments of the basic data were calculated about an arbitrary center of gravity located at 25 percent of the mean aerodynamic chord projected into the plane of symmetry on the thrust line. It was estimated, however, that the addition of the twin-boom assembly would result in a rearward shift in the center of gravity from that used in the all-wing design. Consequently, for the purpose of analyzing the longitudinal stability and control of the twin-boom design, a center-of-gravity location of 23 percent mean aerodynamic chord was chosen for the trim elevator deflection and hinge-moment summary curves. The yawing-moment and trim rudder-deflection summary curves are presented for the 25-percent center-of-gravity position inasmuch as they would be affected only slightly by the 2-percent shift.

The basic elevator, rudder, and aileron test data of the twin-boom model are presented with the horizontal stabilizer set at an angle of 5.4° to the thrust line. The data in the summary analysis related to longitudinal stability and control, however, are presented for a stabilizer setting of 1.4° which, as shown in the stabilizer-effectiveness curves of figure 19, provides trim for zero elevator deflection at an assumed cruising lift coefficient of 0.4.

The flap-deflected tests were run with the plain flap deflected 40°. The flap-effectiveness curves of figure 20 show that the maximum lift coefficient increases with flap deflection, but for deflections greater than 40° there is no further gain in the maximum lift coefficient.

The tests of the all-wing model were conducted at somewhat higher power conditions than those for the twin-boom model; and, therefore, in this comparison analysis, the propeller-operating data of the all-wing tests have been adjusted to the same power or thrust-lift relationship as for the twin-boom tests.

Static Longitudinal Stability and Control

Longitudinal stability.- The stick-fixed neutral-point curves of figure 6 were determined from the pitching-moment lift-coefficient curves of figure 5 by the methods of reference 4. In general, the twin-boom airplane will be about neutrally stable over the lift-coefficient range for a center-of-gravity location at 25 percent mean aerodynamic chord. At the design center-of-gravity location of 23 percent mean aerodynamic chord the airplane will have about a 3-percent static margin in the high-speed range with rated power and about a 5-percent margin at low speed with propellers windmilling and flap deflected 40°. A single instance of a large degree of instability is shown for the flight condition of rated-power operation with the flap deflected 40°. This instability is probably caused by the horizontal tail entering a region of increasing downwash resulting from the combination of the flap deflection and increased slipstream over the wing center section at the high thrust coefficients. As is shown in the section entitled "Performance Estimates," this flap is not an effective high-lift device and also contributes an increment of drag sufficiently high to reduce seriously the climbing ability of the airplane. In low-speed flight with high power, the flap, therefore, would not be deflected; and, accordingly, the longitudinal instability indicated for this flight condition has little significance.

The all-wing model has a similar variation of neutral point with lift coefficient or airspeed and a larger static margin for the rated-power condition. However, in landing attitudes at high angles of attack

with propellers windmilling, the all-wing model shows less static margin. It was found in the tests of the all-wing model that the instability in this condition was associated with extensive trailing-edge separation along the entire span; whereas the lift and stability were maintained for the twin-boom model because the flow in the center section remained undisturbed even at the higher angles of attack (fig. 18).

Although sufficient data are not available for a complete determination of the stick-free neutral points, an indication of the stick-free stability is given by the variation of the pitching-moment coefficient for $C_{h_e} = 0$ with lift coefficient in figure 7. The slopes of the pitching-moment curves for the center of gravity located at 23 percent of the mean aerodynamic chord indicate that the airplane will have about neutral stick-free longitudinal stability for all the conditions investigated. In comparison, the all-wing airplane was longitudinally stable, elevator free, for all power conditions tested.

Longitudinal control.- The variations of elevator deflection for trim with airspeed (fig. 8(b)) indicate that for the center of gravity located at 23 percent mean aerodynamic chord the elevator-deflection range is sufficient to trim the twin-boom airplane for all power conditions tested. All variations are generally stable or neutrally stable except for the condition of rated power with flap deflected which has previously been shown by the neutral-point variation to be longitudinally unstable. The twin-boom airplane possesses less stable trim elevator-deflection variations with airspeed than the all-wing airplane because of the combination of its lower degree of static longitudinal stability and increased elevator effectiveness.

With the tab neutral, the full-scale elevator hinge moments for the twin-boom airplane are comparatively lower (about 1000 lb-ft) with flap retracted but are much greater (up to 3000 lb-ft) with flap deflected than those for the all-wing airplane (fig. 8(b)). The hinge-moment characteristics for the twin-boom airplane in flight and trimmed at specific airspeeds are shown in figure 8(a) to be about neutrally stable in the high-speed range and to have some degree of instability in the very low speed range. The hinge moments for the trimmed conditions are considerably lower than those with the tab neutral.

The values of C_{h_δ} and C_{h_α} for both the twin-boom model and the all-wing model of reference 1 are compared for similar test conditions in the following table:

All-wing airplane			Twin-boom airplane			
α (deg)	C_{h_δ} (per deg)		α (deg)	δ_f (deg)	C_{h_δ} (per deg)	
	Propellers windmilling	Rated power			Propellers windmilling	Rated power
1.3	-0.0071	-0.0095	1.3	0	-0.0130	-0.0115
4.0	-.0063	-.0105	4.0	0	-.0110	-.0117
6.7	-.0059	-.0129	6.7	0	-.0101	-.0109
8.8	-.0064	-.0144	8.8	40	-.0116	-.0143
11.3	-.0075	-.0157	11.3	40	-.0108	-.0148
α (deg)	C_{h_α} (per deg)		α (deg)	δ_f (deg)	C_{h_α} (per deg)	
	Propellers windmilling	Rated power			Propellers windmilling	Rated power
1.3	-0.0032	-0.0046	1.3	0	-0.0021	-0.0016
4.0	-.0030	.0010	4.0	0	-.0031	-.0025
6.7	-.0030	.0034	6.7	0	-.0025	0
8.8	-.0030	-.0003	8.8	40	-.0027	-.0041
11.3	-.0027	-.0012	11.3	40	-.0013	-.0109

The hinge-moment parameters for the twin-boom airplane show that the application of full power has very little effect on C_{h_δ} in the lower angle-of-attack range with the flap retracted. With the flap deflected, however, C_{h_δ} does increase from about -0.0110 to -0.0145 in the high angle-of-attack range with full power. There is, in general, a slight reduction of C_{h_δ} with increase in angle of attack for all conditions of power and flap deflection presented, although for the case with propellers windmilling C_{h_δ} is reduced from -0.0130 to -0.0101 per degree. With the propellers windmilling, the values of C_{h_α} are of the order of -0.0025 and show no consistent variation with angle of attack. The effect of power is to produce values of C_{h_α} less negative for the flap-neutral case but, conversely, to produce a rather large negative increase with the flap deflected 40° (up to -0.0109).

The comparison between the two designs shows that with the propellers windmilling the twin-boom airplane has about a 70-percent increase in the negative values of C_{h_δ}. With rated power, there is very little

variation of C_{h_δ} with α for the twin-boom airplane for a given flap setting, although for the all-wing design, there is a decided increase in C_{h_δ} with angle of attack. The twin-boom airplane has slightly less negative values of C_{h_α} with the propellers windmilling, whereas with rated power applied it has, especially at high angles of attack, more negative values of C_{h_α} than the all-wing design.

The very high negative values of C_{h_δ}, which are characteristic of a plain-flap type of control surface, make this type of control-surface design unsuitable for such a large airplane. In addition to a control surface carefully balanced aerodynamically, which would reduce C_{h_δ} to values of the order of -0.0020, the incorporation of a power-boost system would probably be required to maintain control forces within acceptable limits.

Elevator effectiveness.- The elevator effectiveness for the two airplane designs, as indicated by the relation $dC_m/d\delta_e$, is presented in the following table:

All-wing airplane			Twin-boom airplane			
α (deg)	$dC_m/d\delta_e$ (per deg)		α (deg)	δ_f (deg)	$dC_m/d\delta_e$ (per deg)	
	Propellers windmilling	Rated power			Propellers windmilling	Rated power
1.3	-0.0024	-0.0030	1.3	0	-0.0055	-0.0069
4.0	-.0025	-.0032	4.0	0	-.0055	-.0068
6.7	-.0026	-.0042	6.7	0	-.0056	-.0064
8.8	-.0024	-.0043	8.8	40	-.0070	-.0072
11.3	-.0019	-.0044	11.3	40	-.0068	-.0072

For the twin-boom airplane with propellers windmilling, the effectiveness parameter is essentially a constant value of -0.0055 with flap retracted. Deflection of the flap 40° increases this value to about -0.0069. The effect of applying rated power to the flap-retracted condition is to increase the value of $dC_m/d\delta_e$ from -0.0055 to about -0.0067. Deflection of the flap with rated power increases $dC_m/d\delta_e$ slightly to -0.0072. The twin-boom airplane has approximately twice the elevator effectiveness of the all-wing airplane for the range of test conditions shown.

Static Directional Stability and Control

Directional stability.- From the characteristics of the twin-boom airplane in yaw as summarized in figures 9 to 12, the stability parameters C_{n_ψ}, C_{Y_ψ}, and C_{l_ψ} are obtained and compared with those for the all-wing design in the following table:

Test condition	All-wing airplane				Twin-boom airplane				
	α (deg)	C_{n_ψ} (per deg)	C_{Y_ψ} (per deg)	C_{l_ψ} (per deg)	α (deg)	δ_f (deg)	C_{n_ψ} (per deg)	C_{Y_ψ} (per deg)	C_{l_ψ} (per deg)
Propellers windmilling	4.8	-0.00040	0.0045	0.00022	4.8	40	-0.00045	0.0035	-0.00036
	7.6	-.00040	.0045	.00022	7.6	40	-.00051	.0035	-.00026
	11.4	-.00041	.0045	.00024	11.4	40	-.00060	.0033	0
	15.2	-.00042	.0046	.00033	15.2	40	-.00068	.0031	.00100
Rated power	1.2	-.00039	.0045	.00036	1.2	0	-.00050	.0040	-.00021
	3.5	-.00042	.0047	.00020	3.5	0	-.00053	.0040	-.00034
	5.8	-.00044	.0051	.00014	5.8	0	-.00059	.0042	-.00019
	8.5	-.00044	.0058	.00019	8.5	0	-.00069	.0046	-.00040
Asymmetric power	4.9	-.00039	.0053	.00013	4.9	0	-.00061	.0038	-.00018
	6.7	-.00046	.0055	.00007	6.7	0	-.00068	.0041	-.00020
	9.5	-.00050	.0057	0	9.5	0	-.00071	.0041	-.00015
	12.2	-.00051	.0058	-.00003	12.2	0	-.00078	.0040	-.00005

The slopes in the table indicate the characteristics of the models for zero yaw but also represent the characteristics over the entire yaw range because of the linear variation of C_n, C_l, and C_Y with ψ shown in figure 9. The directional stability of the twin-boom

design is shown to be very low with C_{n_ψ} ranging from a minimum value of -0.00045 with propellers windmilling to a maximum value of -0.00078 with asymmetric power. There is an increase in C_{n_ψ} with increased angle of attack. Although these values of C_{n_ψ} are quite low for the twin-boom design they are approximately 45 percent greater than those for the all-wing airplane.

The application of high power produces a positive side-force increment, and, as shown in the table, increases the value of C_{Y_ψ} from 0.0031 with propellers windmilling to 0.0046 for rated power at the highest angle of attack investigated for the two power conditions. The lateral force developed by the twin-boom design ranges from 10 to 30 percent less than that produced by the all-wing airplane. The lateral-force characteristics that would occur with the airplane trimmed directionally (fig. 10) show only slightly stable C_Y variations against angle of yaw. The maximum value of $C_{Y_{\psi_{trim}}}$ of 0.0010 is about one-half that for the all-wing airplane.

The dihedral effect for the twin-boom model is very low and of small negative value. This condition should be expected since the wing possesses a small amount of negative geometric dihedral. The values of C_{l_ψ}, as indicated in the table, show no systematic variation with angle of attack or power and are about -0.00020 for all conditions tested, except for propellers windmilling at the highest angle of attack where C_{l_ψ} is 0.00100. Except for this stalled angle of attack, the effective dihedral angle ranges from about 0° to -2° for the conditions investigated. The higher degree of positive dihedral effect at the highest angle of attack is explained by the combined effect of yaw and negative dihedral which increases effectively the angle of attack and thereby induces stall on the trailing wing and produces a positive dihedral effect. The tendency for the wing to roll to the left at zero yaw as the angle of attack is increased (fig. 9) is caused by the greater area of stall on the left wing panel shown by the stall progressions of figure 18. For the most part the effective dihedral is nearly the same for both the designs except for the change in sign resulting from the opposite geometric dihedral used for the two wings.

The aileron characteristics for the twin-boom airplane (fig. 29) are very similar to those of the all-wing configuration in that the rate of change of rolling moment with aileron deflection is nearly linear up to aileron deflections of about 20°. At higher aileron deflections, aileron stall causes a reduction of effectiveness for both airplanes. It is estimated that the rolling moments developed with the twin-boom airplane yawed 15° can be trimmed out by aileron deflections of about 5°.

The pitching-moment coefficients are essentially constant in the yaw range between $\pm 10^{\circ}$ for the angle-of-attack range and power conditions investigated (fig. 11). A rapid destabilizing pitching-moment trend is shown above 10° yaw which becomes very pronounced at the highest angle of attack for each power condition. The cause for this longitudinal instability is not clear from the data available, but it is possible that at the high angles of attack and high angles of yaw the wing and boom wakes may have incurred some loss of lift at the horizontal tail. The loss of the slipstream of the left outboard propeller for the asymmetric-power case appears to aggravate this nose-up pitching tendency, which indicates the presence of poor flow that is partially controlled by the propeller slipstream. There is some reduction in the lift coefficient shown in figure 12 as the yaw angle is increased; consequently, there is justification for assuming that the loss in lift at the tail is a contributing factor inasmuch as the wing itself is not sufficiently stalled to produce such a severe pitching tendency at the angles of attack considered. An elevator deflection of approximately 5° offsets any pitching moment due to angle of attack or power variation over a yaw range from -10° to 12°. Higher positive yaw angles introduce undesirable longitudinal control characteristics but, since the trimmed yaw range never exceeds 10°, the significance of this longitudinal instability is decreased.

Directional control.- The rudder deflections required to trim the airplane directionally at zero yaw are shown in figure 13 to vary from about 2° left to 10° right for the flight conditions investigated. With the propellers windmilling there is no variation of trim rudder deflection with airspeed. For the other power conditions the trim rudder deflections increase to the right continuously with decreased airspeed.

The variations of trim rudder hinge moment with airspeed show that for the propellers-windmilling flap-retracted condition there is zero hinge moment throughout the speed range. For all other conditions of power and flap deflection the hinge-moment variations are such that increasing right pedal forces would be required with the rudder deflections to the right as the airspeed is decreased. These variations are an improvement over the wide range of forces that was found in an unpublished analysis to be required to trim, directionally, the all-wing airplane.

The hinge-moment variations with rudder deflection in figure 30 show continuous and smooth curves of C_{h_r} against δ_r over the complete deflection range. In the low deflection range of $\pm 10^{\circ}$, however, the slope of the hinge-moment curve is about one-half that in the higher deflection range. A comparison of the rudder hinge-moment characteristics for the twin-boom and the all-wing airplanes is given in the following table:

Test condition	All-wing airplane		Twin-boom airplane		
	α (deg)	$dC_{h_r}/d\delta_r$ (per deg)	α (deg)	δ_f (deg)	$dC_{h_r}/d\delta_r$ (per deg)
Propellers windmilling	2.1	-0.0047	2.1	0	-0.0020
	4.9	-.0052	4.9	0	-.0020
	7.7	-.0056	7.7	0	-.0020
	10.4	-.0060	10.4	40	-.0016
	12.3	-.0061	12.3	40	-.0016
	15.2	-.0061	15.2	40	-.0016
Rated power	1.2	-.0040	1.2	0	-.0030
	3.1	-.0046	3.1	0	-.0028
	5.8	-.0058	5.8	0	-.0026
	8.4	-.0071	8.4	40	-.0039
	11.2	-.0081	11.2	40	-.0040
Asymmetric power	4.9	-.0052	4.9	0	-.0033
	6.7	-.0056	6.7	0	-.0032
	9.4	-.0061	9.4	0	-.0029
	12.2	-.0065	12.2	0	-.0027

For the twin-boom airplane, angle of attack has very little effect on the rudder hinge moments, but about a 55-percent increase results from application of rated power and a 30-percent further increase results at rated power with the flaps deflected 40°. For the conditions investigated, $dC_{h_r}/d\delta_r$ values range from -0.0016 to -0.0040. For the all-wing airplane, with the rudders located at the wing trailing edge, $dC_{h_r}/d\delta_r$ increased with increased angle of attack and with power at high angles of attack. For the all-wing design, the slopes range from -0.0040 to about -0.0080, or nearly double those of the twin-boom airplane.

The power of the rudder to trim the airplane in yaw is shown in figure 10 to be rather low. In the small range of yaw between ±4° the rudder deflection required for trim is about 2° per degree of yaw. For yaw angles greater than ±4°, however, large increases in the rudder deflection are necessary to trim out small increments of yaw, such that at the maximum deflection of the rudders to the right (-30°) the limiting trimmed yaw attitude is 8.5° with propellers windmilling near the stalling angle of attack. Application of rated and asymmetric power increases the trim-deflection angle to the right at zero yaw and consequently

decreases the range of sideslip to the right, although essentially the same characteristic trends of δ_r with ψ are observed as for the propellers-windmilling condition. These results are very similar to those of the tests of the all-wing airplane except that the rudders were capable of trimming the all-wing airplane to angles of yaw from 2° to 5° higher. The large rudder deflections required in yaw will result in very high rudder hinge moments which will require a power-boost system to produce pedal forces within acceptable limits.

Rudder effectiveness.- In the curves of trim rudder deflection against yaw the power of the rudder was shown to be quite low, especially in the deflection range greater than about ±10°. The characteristics of the rudder in the low deflection range are indicated by the parameters $dC_n/d\delta_r$ and $dC_Y/d\delta_r$ in the following table for both the twin-boom and the all-wing airplanes.

Test condition	All-wing airplane			Twin-boom airplane			
	α (deg)	$dC_n/d\delta_r$ (per deg)	$dC_Y/d\delta_r$ (per deg)	α (deg)	δ_f (deg)	$dC_n/d\delta_r$ (per deg)	$dC_Y/d\delta_r$ (per deg)
Propellers windmilling	2.1	-0.00029	0.0028	2.1	0	-0.00015	0.0014
	4.9	-.00023	.0024	4.9	0	-.00015	.0014
	7.7	-.00020	.0023	7.7	0	-.00015	.0014
	10.4	-.00021	.0023	10.4	40	-.00026	.0013
	12.3	-.00022	.0022	12.3	40	-.00026	.0013
	15.2	-.00022	.0021	15.2	40	-.00026	.0013
Rated power	1.2	-.00027	.0025	1.2	0	-.00028	.0016
	3.1	-.00026	.0027	3.1	0	-.00029	.0015
	5.8	-.00031	.0032	5.8	0	-.00029	.0017
	8.4	-.00037	.0038	8.4	40	-.00033	.0016
	11.2	-.00040	.0040	11.2	40	-.00033	.0018
Asymmetric power	4.9	-.00026	.0027	4.9	0	-.00031	.0014
	6.7	-.00028	.0028	6.7	0	-.00032	.0015
	9.4	-.00030	.0029	9.4	0	-.00034	.0015
	12.2	-.00030	.0031	12.2	0	-.00036	.0016

For the rudder-neutral zero-yaw condition the two airplane designs have approximately the same degree of rudder effectiveness, with the greatest variation shown for the propellers-windmilling flap-retracted

condition. Values of $dC_n/d\delta_r$ range from -0.00015 to -0.00040 for all the conditions investigated. The effectiveness of the rudders is increased nearly twofold by propeller operation at rated power and by deflection of the flap with the propellers windmilling. The reduction in rudder effectiveness in the high deflection range (figs. 27 and 28) is attributed to separation occurring over the control surfaces at high angles of attack.

The side-force variation $(dC_Y/d\delta_r)$ for the twin-boom model shows very little variation with angle of attack, flap deflection, or power and has an average value of about 0.0015 which is approximately one-half that shown for the all-wing airplane. As in the case of the yawing moments, there is an appreciable reduction in the slope of the curve of lateral-force coefficient against rudder deflection as the rudders are deflected beyond $\pm 10^{\circ}$ (figs. 27 and 28).

Performance Estimates

The results of the present series of tests and the tests of reference 1 offer an opportunity to compare the performance of these two airplanes. The data show that the stability and control characteristics of the airplanes are similar so that they should represent directly comparable airplanes for such an analysis.

The lift and drag data, however, indicate that, although a performance comparison can be made for these specific airplanes, no general conclusions as to the relative performance of the two types may be made. Comparisons of the curves of lift coefficient against longitudinal-force coefficient for the propellers-removed, propellers-windmilling, and rated-power conditions are shown in figure 14. With propellers removed, the basic drag coefficient of the twin-boom airplane is about 0.0050 higher than the all-wing airplane in the range of C_L from 0.2 to 0.8. At lift coefficients greater than about 0.95, however, the drag coefficient of the all-wing airplane is greater than that for the twin-boom airplane because of the greater angle of attack required to maintain the same lift coefficient. With the propellers installed and windmilling, the drag of the all-wing airplane is greater than that for the twin-boom airplane above lift coefficients of about 0.5 and is essentially the same at lower lift coefficients. The curves of lift coefficient against longitudinal-force coefficient for the rated-power condition show a similar trend, thus greater excess thrust is provided for the twin-boom airplane at the higher lift coefficients. There is evidently an adverse effect of the tractor-propeller configuration on the drag characteristics of the all-wing airplane. The performance characteristics of these specific airplanes should not, therefore, be regarded as indicative of the relative performance of the general types of tail-boom and all-wing airplanes.

The trimmed maximum lift coefficient with the propellers windmilling is increased from about 1.03 for the all-wing airplane to about 1.31 for the twin-boom airplane with the flap deflected 40°. As described previously, the wing of the all-wing configuration, having an upward reflexed trailing edge, was inverted and used for the twin-boom design; and thereby some additional camber was introduced into the wing by directing the reflex of the trailing edge downward. Thus the greatest contributing factor toward increasing the maximum lift coefficient from 1.03 to 1.31 is the increased effective camber of the wing and, to a lesser extent, the flap deflection of 40°. The increase in $C_{L_{max}}$ represents an appreciable reduction in the stalling speed at sea level from 92 to 82 miles per hour. The top speed of each airplane with rated-power operation is about 200 miles per hour.

In order to facilitate the performance estimates of the two designs, comparisons of the drag coefficients are presented with controls neutral inasmuch as the drag of deflected controls (figs. 15 and 16) is small in the low deflection range required for trim. The variations of drag coefficient or longitudinal-force coefficient with airspeed for the propellers-windmilling and rated-power conditions are given in figure 17. As previously discussed, the two airplanes have nearly the same drag below a lift coefficient of about 0.5 or above a speed of 130 miles per hour, but there is less drag and therefore an excess of thrust for the twin-boom airplane at speeds below 130 miles per hour. The twin-boom airplane, therefore, will have improved take-off and landing performance but will have essentially the same range and rate of climb as the all-wing airplane.

The values of the ratio of maximum lift coefficient to longitudinal-force coefficient increase from about 19 with propellers windmilling to about 23.5 at rated power for both designs at a lift coefficient of 0.45 or a speed of about 140 miles per hour. The estimated range for each airplane, therefore, based on a cruising speed of 140 miles per hour and a fuel capacity of 6000 gallons, is about 3500 miles. The maximum rate of climb for each airplane is estimated to be about 600 feet per minute at a flight speed of about 135 miles per hour. The take-off run for each airplane was computed assuming a level field, no wind, and a take-off speed of 100 miles per hour. On this basis it is estimated that the twin-boom airplane will require a 4100-foot take-off run, which is about 7 percent less than that for the all-wing airplane. Also, to clear a 50-foot obstacle on take-off the twin-boom airplane will require a distance of about 4900 feet, which is approximately 9 percent less than that for the all-wing airplane.

The excessive distances required for take-off, the low rates of climb, and the low cruising and maximum speeds all show clearly that these airplanes are underpowered. An analytical study (reference 5)

of the comparative performance of different types of airplanes shows that, for an all-wing airplane, the minimum total power necessary to provide an adequate margin of economy and performance is of the order of 21,000 brake horsepower, which is an increase of about threefold that used for the designs in this investigation.

SUMMARY OF RESULTS

An investigation of a $\frac{1}{7}$-scale powered model of a twin-boom airplane has been made to obtain a comparison of its stability, control, and performance characteristics with those of an all-wing model of similar proportions previously investigated. The significant results of the investigation are summarized as follows:

1. At the design center-of-gravity location of 0.23 mean aerodynamic chord, the twin-boom airplane had about a 3-percent static margin in the high-speed range with rated power and about a 5-percent static margin at low speed with propellers windmilling and flap deflected 40°. In comparison, the all-wing airplane had a somewhat larger static margin for rated-power operation but much less static longitudinal stability at low speeds with propellers windmilling.

2. The twin-boom airplane possessed generally stable or neutrally stable variations of trim elevator deflection with airspeed for all conditions except for rated power with the flap deflected. The twin-boom airplane had less stable trim elevator-deflection variations with airspeed than the all-wing airplane because of the combination of the lower degree of static longitudinal stability and increased elevator effectiveness. In general, the twin-boom airplane had neutrally stable trim elevator hinge-moment variations with airspeed as compared with the more stable variations for the all-wing airplane.

3. The elevators for both the twin-boom and all-wing designs had values of C_{h_α}, the variation of hinge moment per degree angle of attack, of about -0.0025 per degree with propellers windmilling but the twin-boom configuration had greater negative values (up to -0.0109) with rated power. The twin-boom airplane had values of C_{h_δ}, the variation of hinge moment per degree elevator deflection, ranging from -0.0110 to -0.0145 per degree with rated-power operation and from -0.0130 to -0.0101 per degree with the propellers windmilling for the conditions investigated. The all-wing airplane had comparable values of C_{h_δ} with rated-power operation but had C_{h_δ} values about 70 percent lower with the propellers windmilling.

4. The elevator-effectiveness parameter of the twin-boom airplane ranged from -0.0055 to -0.0072 per degree for all conditions tested and was about twice that of the all-wing configuration.

5. The twin-boom airplane had static directional stability with rudders fixed, with the directional-stability parameter ranging from -0.00045 to -0.00078 per degree for the conditions tested. Although these values were low, they were about 45 percent greater than those determined for the all-wing airplane.

6. The side force developed by the twin-boom airplane in yaw was very low and was approximately one-half that for the all-wing airplane.

7. The effective dihedral angles for both the all-wing and twin-boom airplanes ranged from 0° to $\pm 2^{\circ}$ for angles of attack below the stall.

8. Both the twin-boom and all-wing airplane had stable or at least neutrally stable trim rudder-deflection and hinge-moment variations with airspeed. The all-wing airplane, however, had an undesirable power effect on the rudder characteristics. The values of the rudder hinge-moment parameter C_{h_δ} for the twin-boom airplane, which ranged from -0.0016 to -0.0040 per degree, were about one-half those for the all-wing airplane.

9. The power of the rudder to trim the twin-boom airplane in yaw was low. In the landing attitude with propellers windmilling, maximum rudder deflection of -30° would trim only 8.5° of yaw. The rudders of the all-wing airplane provided a trimmed yaw range from 2° to 5° greater than that for the twin-boom airplane.

10. The rudder effectiveness was approximately the same for both designs investigated in the low rudder-deflection range with values of the rudder-effectiveness parameter ranging from -0.00015 to -0.00040 per degree for the conditions tested.

11. The maximum trimmed lift coefficient for the twin-boom airplane was 1.31 compared with 1.03 for the all-wing airplane, and gave a reduction in stalling speed of from 92 to 82 miles per hour. This increase in maximum lift coefficient for the twin-boom airplane was accomplished largely by the increased effective camber of the wing resulting from a downward reflexed trailing edge. The indicated top level-flight speed of each airplane at sea level with rated power was about 200 miles per hour.

12. The twin-boom airplane will have about a 7 percent shorter take-off run and will require about 9 percent less distance to clear a 50-foot

obstacle than the all-wing airplane. Both airplanes have essentially the same performance in range and rate of climb.

Langley Aeronautical Laboratory
National Advisory Committee for Aeronautics
Langley Field, Va., March 23, 1948

REFERENCES

1. Brewer, G. W., and Rickey, E. A.: Tests of a 1/7-Scale Powered Model of the Kaiser Tailless Airplane in the Langley Full-Scale Tunnel. NACA MR No. L6C13, 1946.

2. DeFrance, Smith J.: The N.A.C.A. Full-Scale Wind Tunnel. NACA Rep. No. 459, 1933.

3. Theodorsen, Theodore, and Silverstein, Abe: Experimental Verification of the Theory of Wind-Tunnel Boundary Interference. NACA Rep. No. 478, 1934.

4. Schuldenfrei, Marvin: Some Notes on the Determination of the Stick-Fixed Neutral Point from Wind-Tunnel Data. NACA RB No. 3I20, 1943.

5. Ankenbruck, Herman O., and McKinney, Marion O., Jr.: Generalized Performance Comparison of Large Conventional, Tail-Boom, and Tailless Airplanes. NACA TN No. 1477, 1947.

TABLE I

PHYSICAL AND DIMENSIONAL CHARACTERISTICS OF SIMILAR ALL-WING

AND TWIN-BOOM AIRPLANES BASED ON $\frac{1}{7}$- SCALE MODELS

	All-wing airplane	Twin-boom airplane
Design gross weight, lb	175,000	177,500
Wing:		
Area, sq ft	7920	7920
Span, ft	290	290
Mean aerodynamic chord, ft	27.3	27.3
Location of mean aerodynamic chord behind root chord leading edge, ft	1.74	1.74
Aspect ratio	10.6	10.6
Taper ratio	0.20	0.20
Root section (symmetrical to 0.85c')	NACA 63,4-020	NACA 63,4-020
Tip section (symmetrical to 0.85c')	NACA 65,3-018	NACA 65,3-018
Trailing-edge reflex modification behing 0.85c'	Upward	Downward
Dihedral, outer panel, deg	1.7	-1.7
Wing twist, deg	0	0
Sweepback of 20-percent-chord line, deg	0	0
Wing loading, lb/sq ft	22.1	22.4
Horizontal tail:		
Total area, sq ft	----------	406
Elevator area behind hinge line, sq ft	193	203
Elevator balance, percent	12.7	9.8
Span, ft	48.2	44.9
Root-mean-square chord, ft	4	4.51
Hinge line, percent wing chord	90	----------
Hinge line, percent stabilizer chord	----------	50
Maximum deflection, deg	10, -30	10, -30
Vertical tail:		
Total area, sq ft	820	400
Rudder area behind hinge line, sq ft, total	267	137
Rudder balance, percent	12.5	10.9
Vertical-tail height above wing trailing edge, ft	19.8	28.8
Root-mean-square rudder chord, ft	3.02	3.18
Hinge line, percent of fin chord	70	70
Maximum deflection, deg	±30	±30
Aileron:		
Area behind hinge line, each, sq ft	277	277
Aileron balance, percent	15.4	15.4
Span, ft	90	90
Root-mean-square chord, ft	3.24	3.24
Hinge line, percent wing chord	85	85
Maximum deflection, deg	10, -30	10, -30
Flap:		
Span, ft	----------	39
Chord, ft	----------	5.25
Propeller:		
Designation	Hamilton Standard 6491A-0	Hamilton Standard 6491A-0
Diameter, ft	15.167	15.167
Number of blades	4	4
Gear ratio	0.45	0.45

NACA

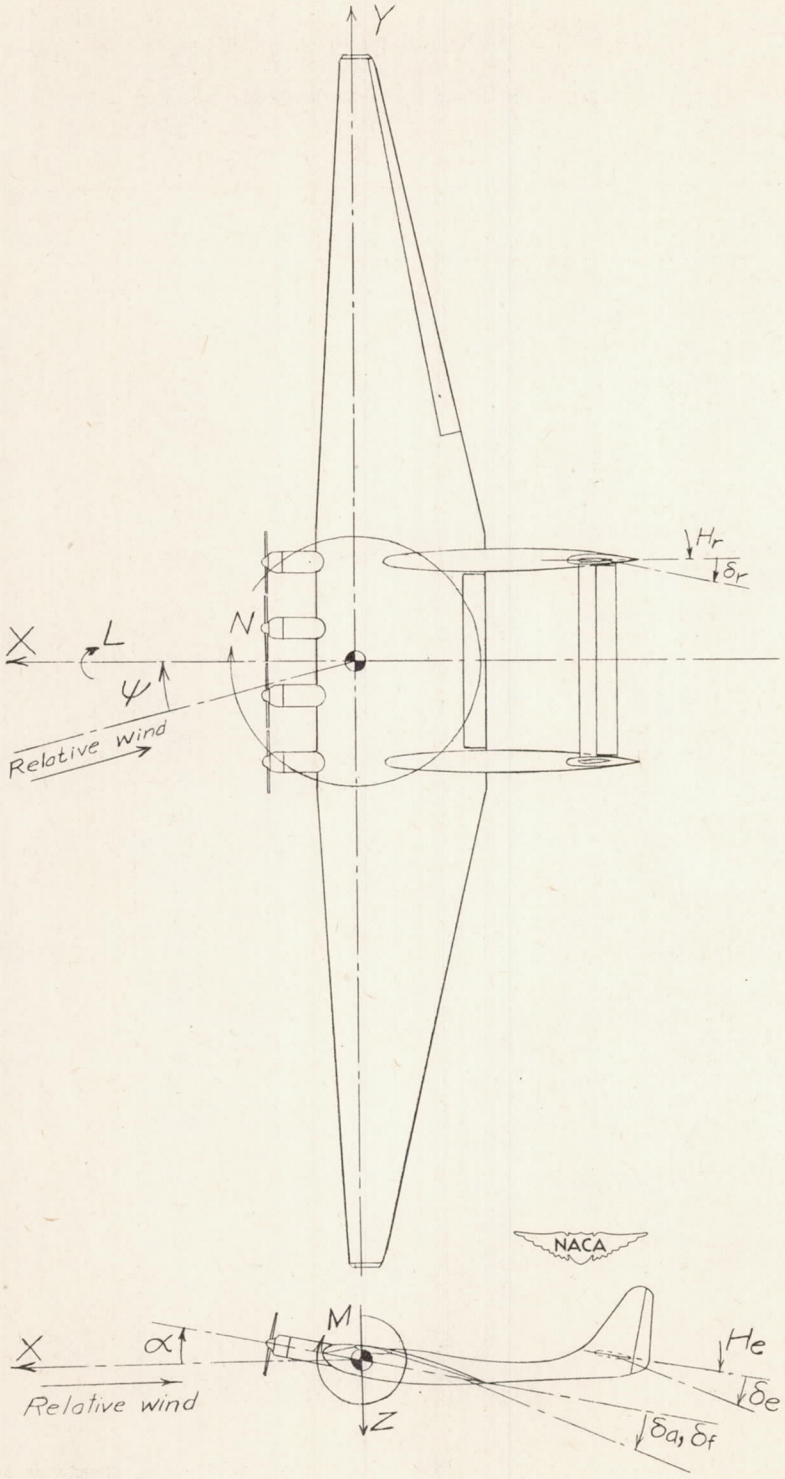

Figure 1.- System of axes and control-surface hinge moments and deflections. Positive directions of forces, moments, and angles are indicated by arrows.

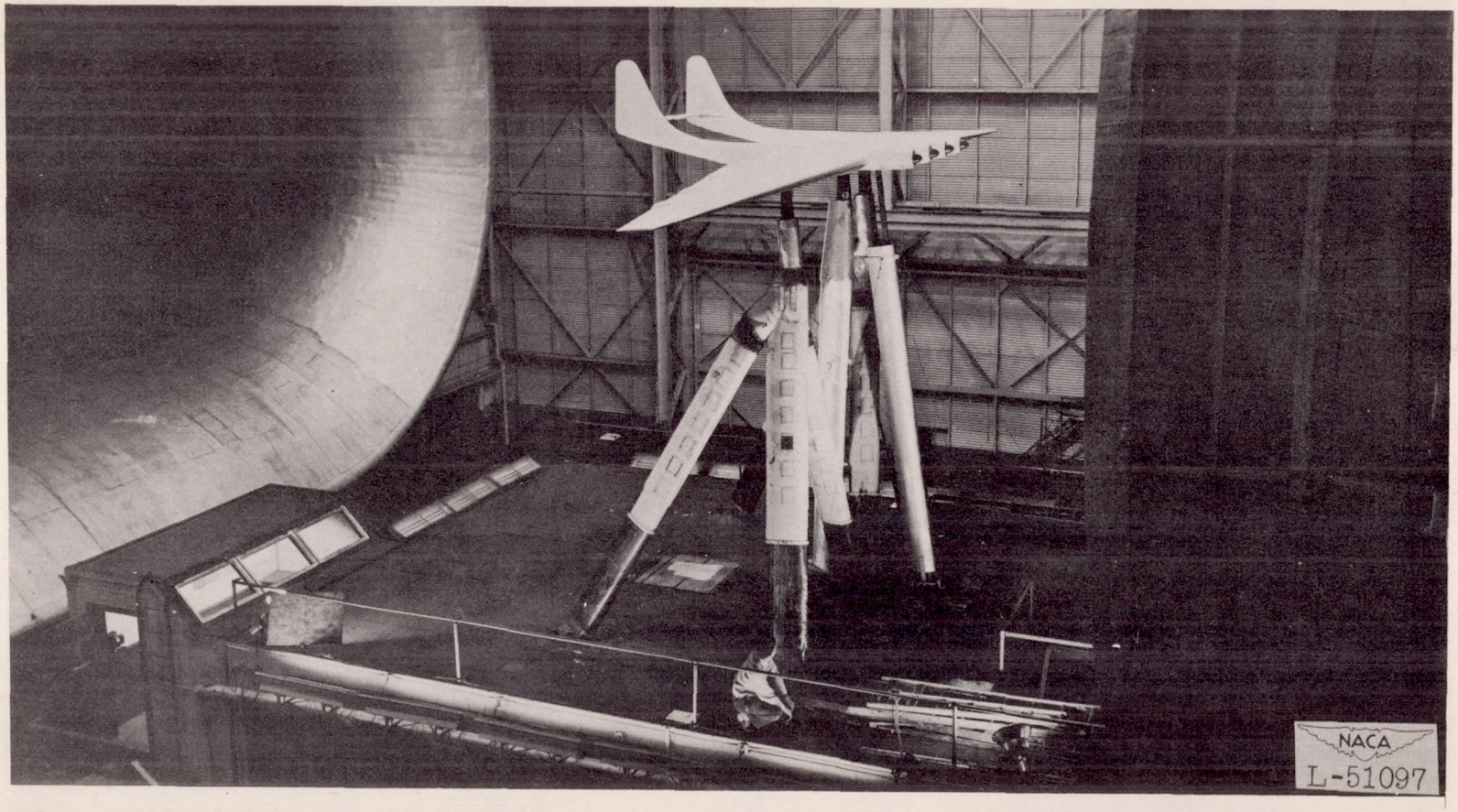

(a) Three-quarter front view; propellers removed; tare dummy strut installed.

Figure 2.- The $\frac{1}{7}$-scale model of a twin-boom airplane mounted for test in the Langley full-scale tunnel.

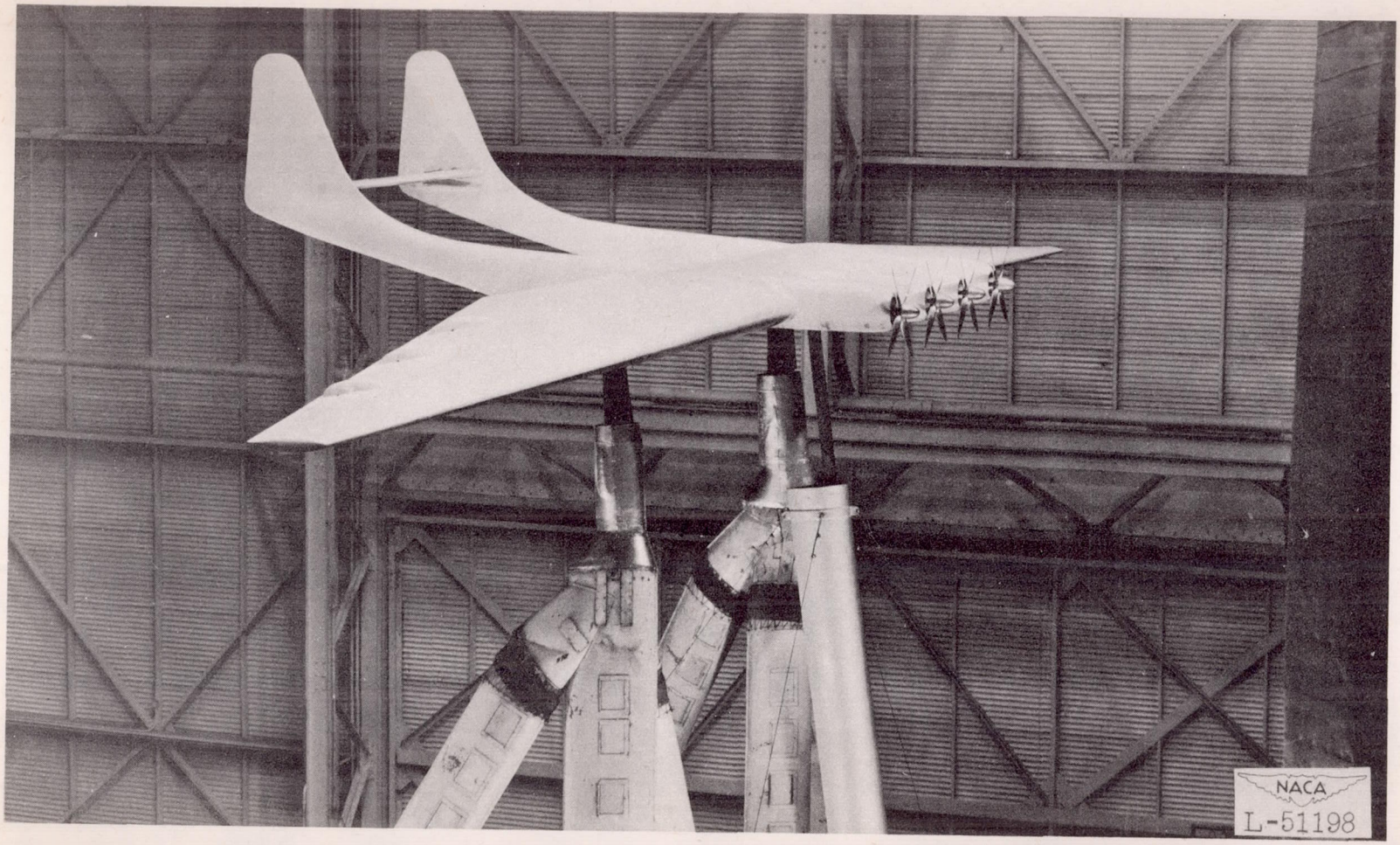

(b) Three-quarter front view; propellers installed.

Figure 2.- Continued.

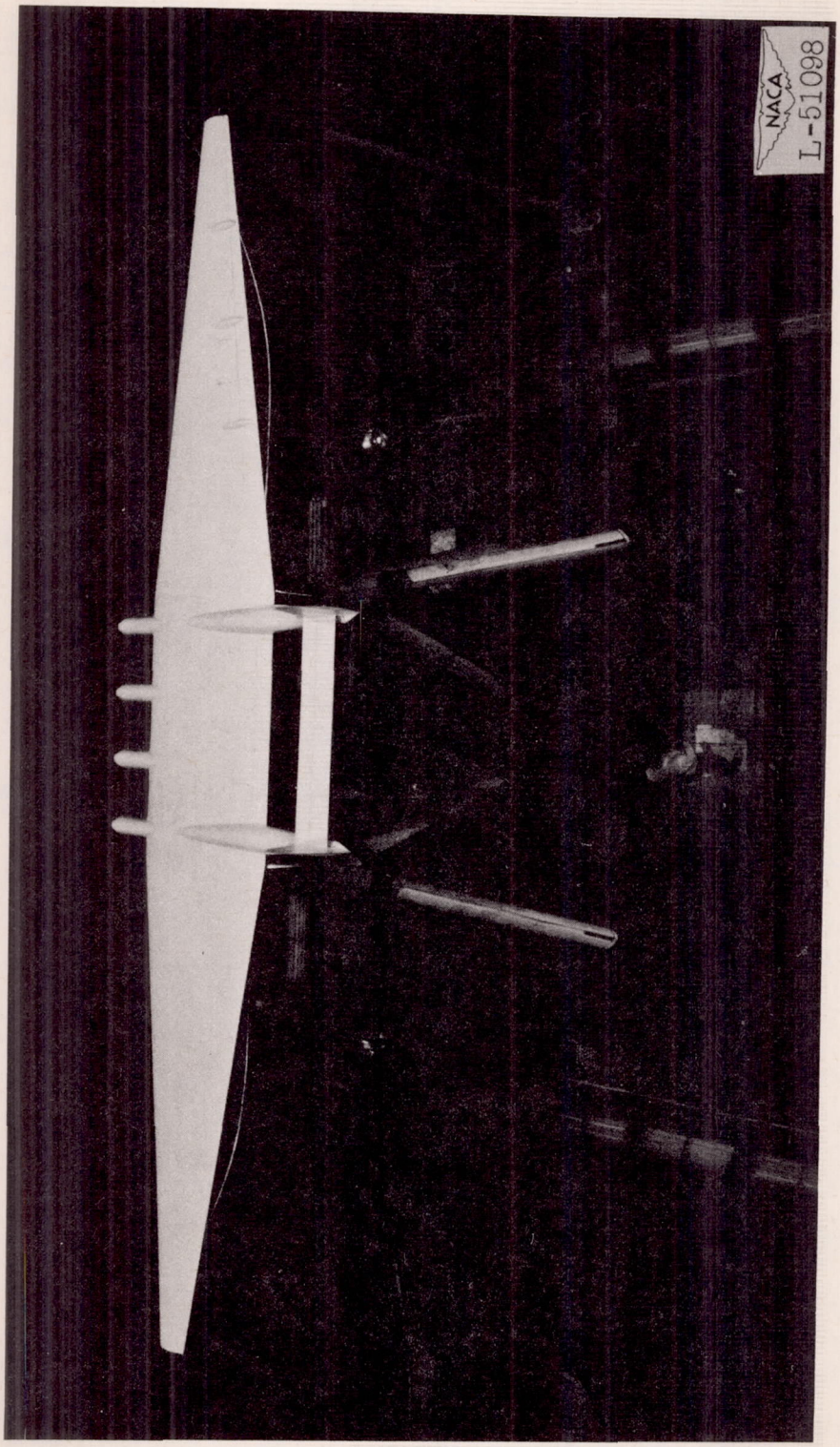

(c) Rear view; propellers removed.

Figure 2.- Concluded.

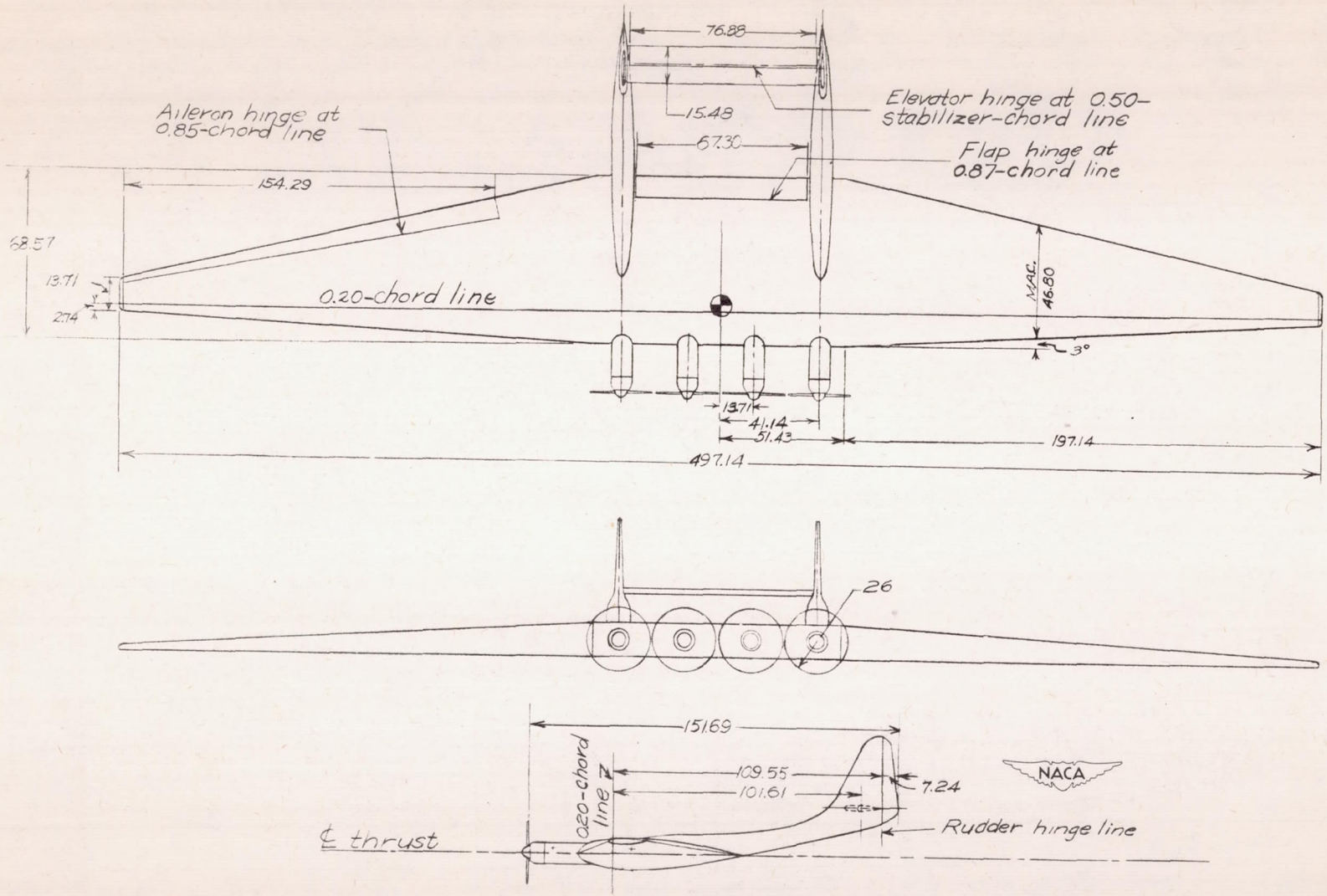

(a) Twin-boom model.

Figure 3.- Three-view drawings of the $\frac{1}{7}$-scale models tested in the Langley full-scale tunnel. (All dimensions are in inches.)

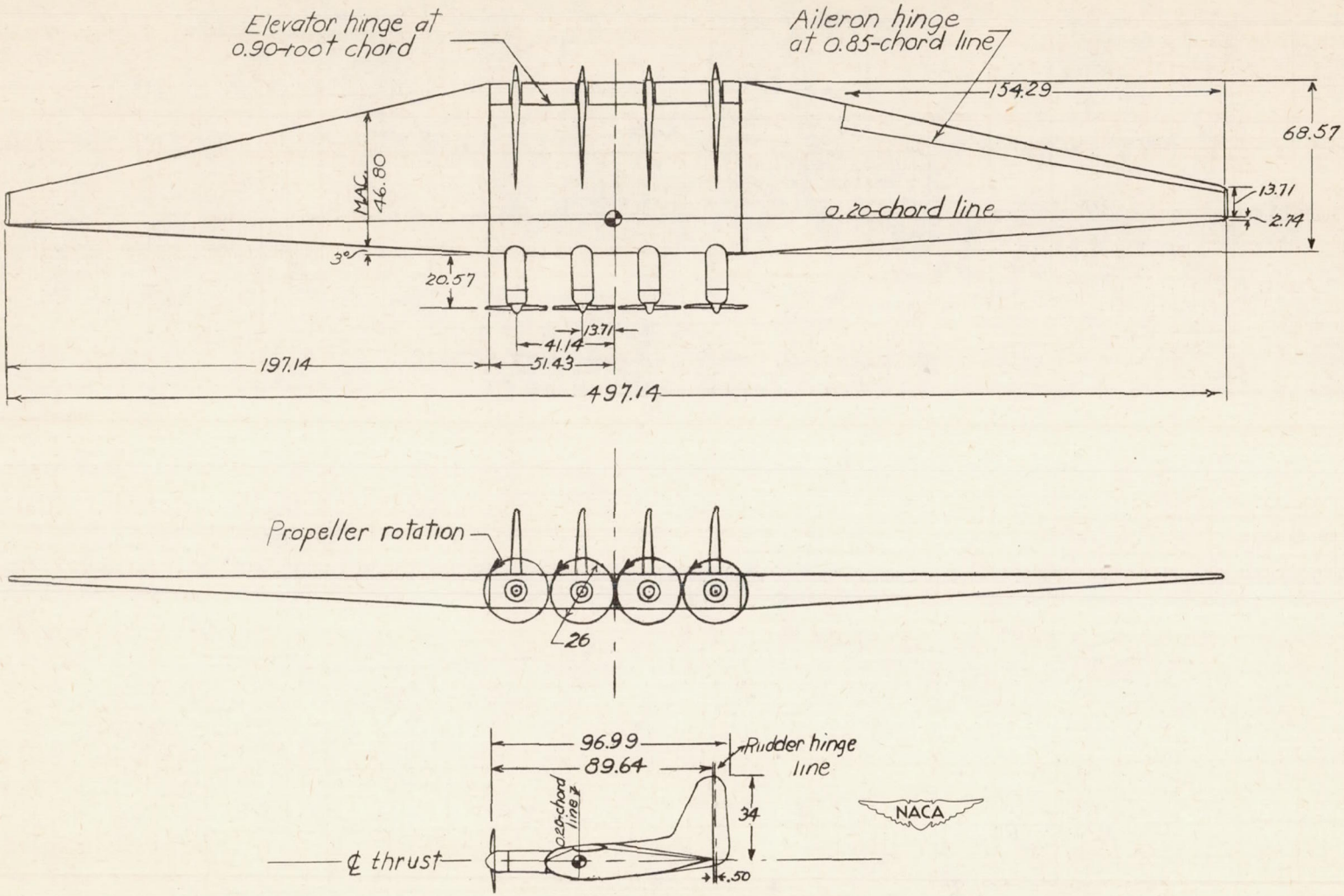

(b) All-wing model.

Figure 3.- Concluded.

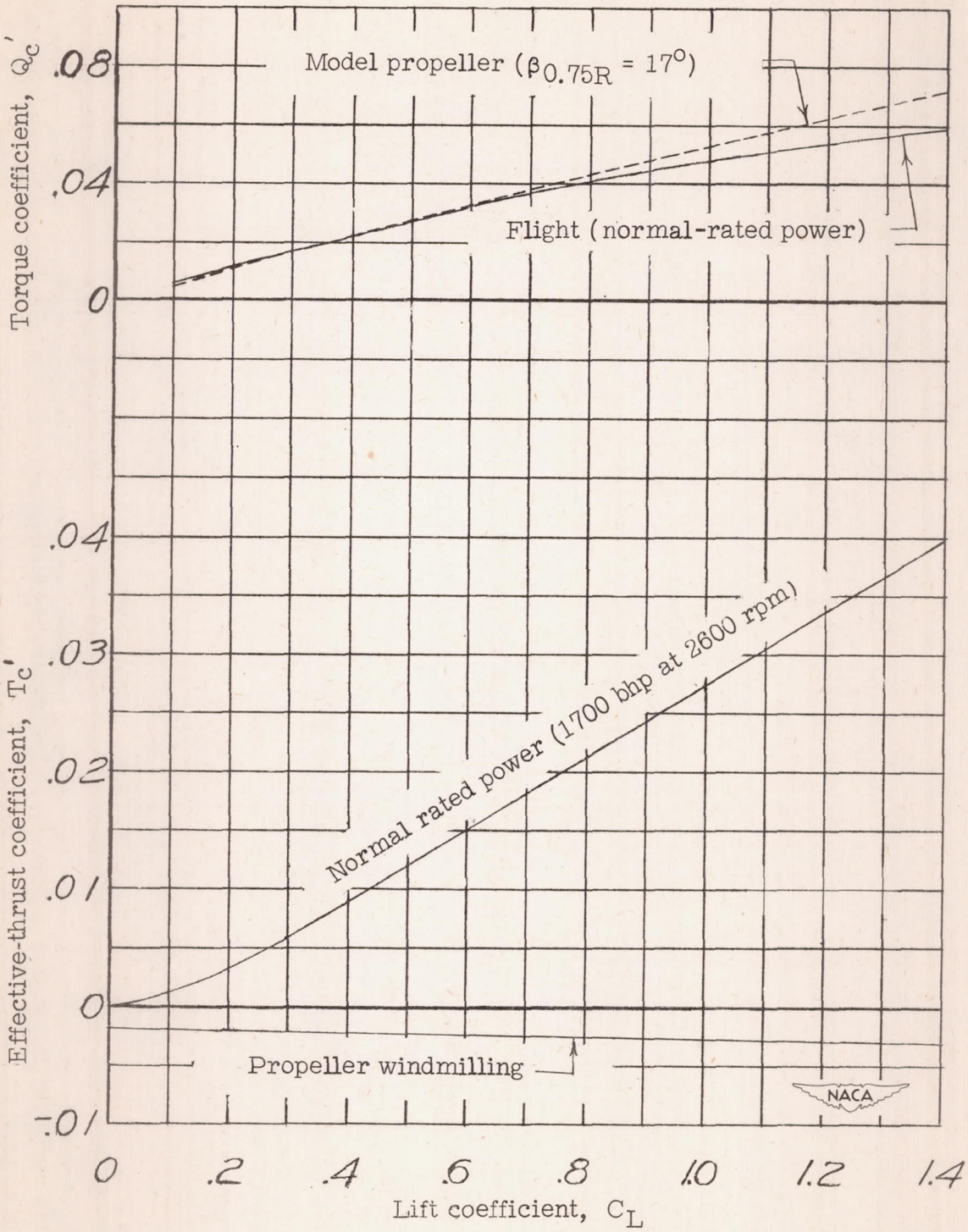

Figure 4.- Variation of effective-thrust coefficient and torque coefficient with lift coefficient for a single propeller. Sea-level operation; $\frac{W}{S}$ = 22.4 pounds per square foot.

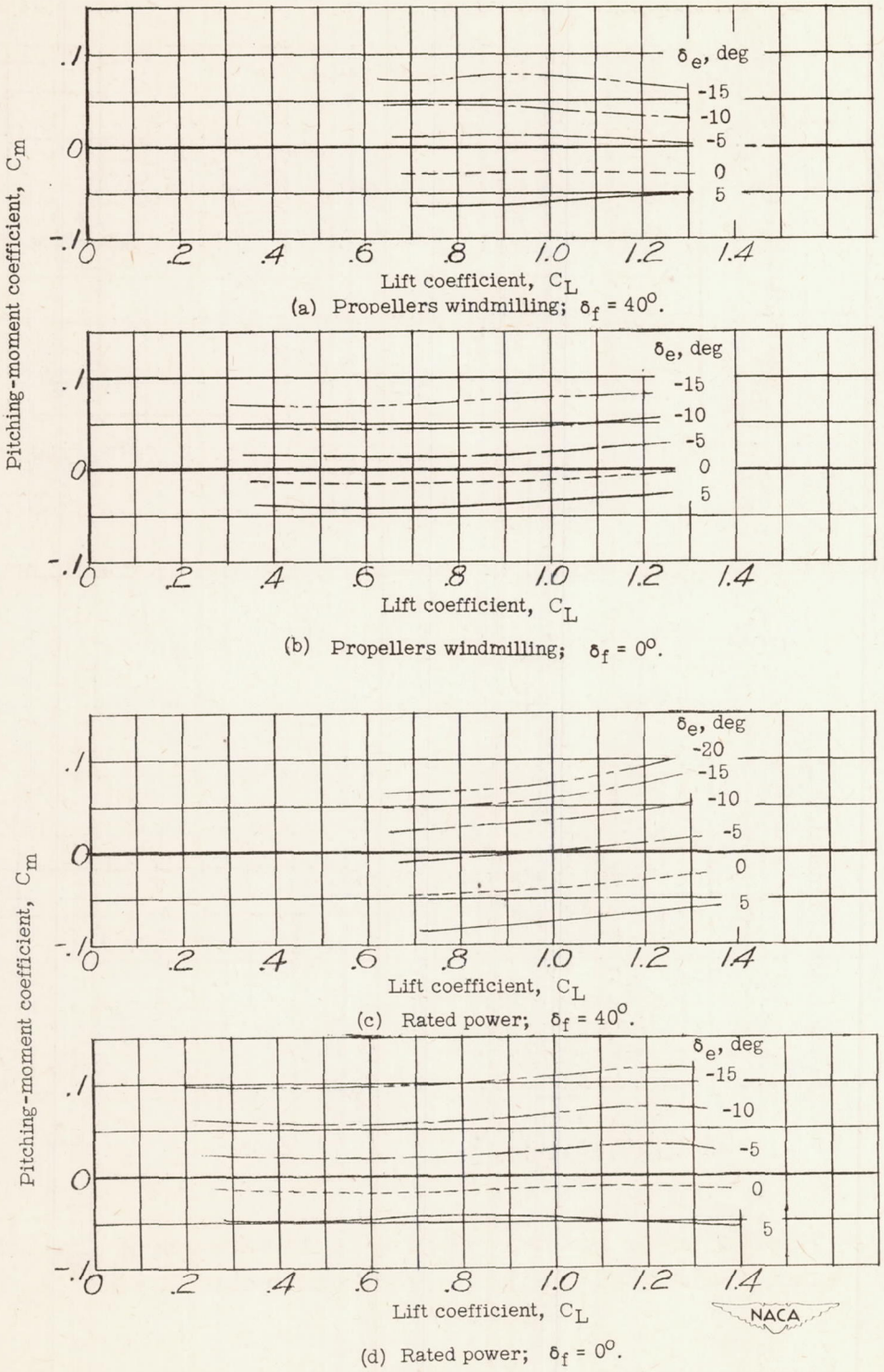

Figure 5.- Effect of power and flap deflection on the variation of C_m with C_L. Stick fixed; center of gravity at 0.25 mean aerodynamic chord; $i_t = 1.4^\circ$; $\delta_a = 0^\circ$; $\delta_r = 0^\circ$.

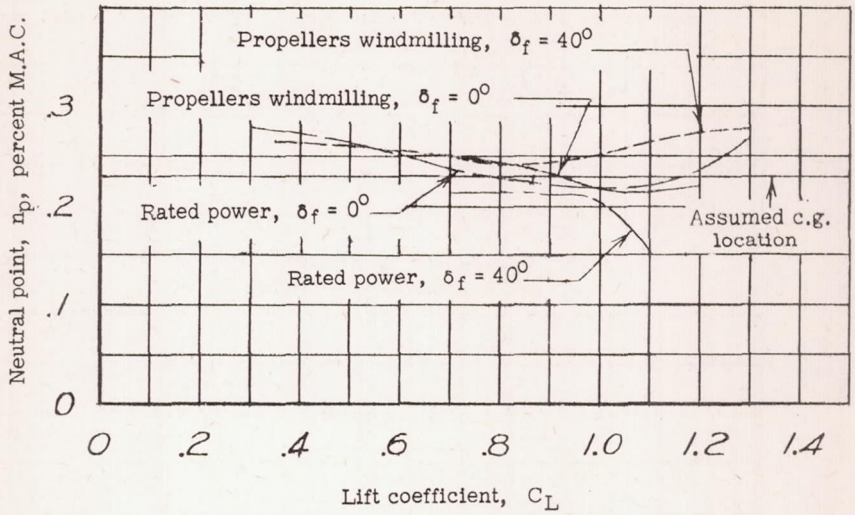

Figure 6.- Variation of stick-fixed neutral point with lift coefficient. $i_t = 1.4^\circ$; $\delta_a = 0^\circ$; $\delta_r = 0^\circ$.

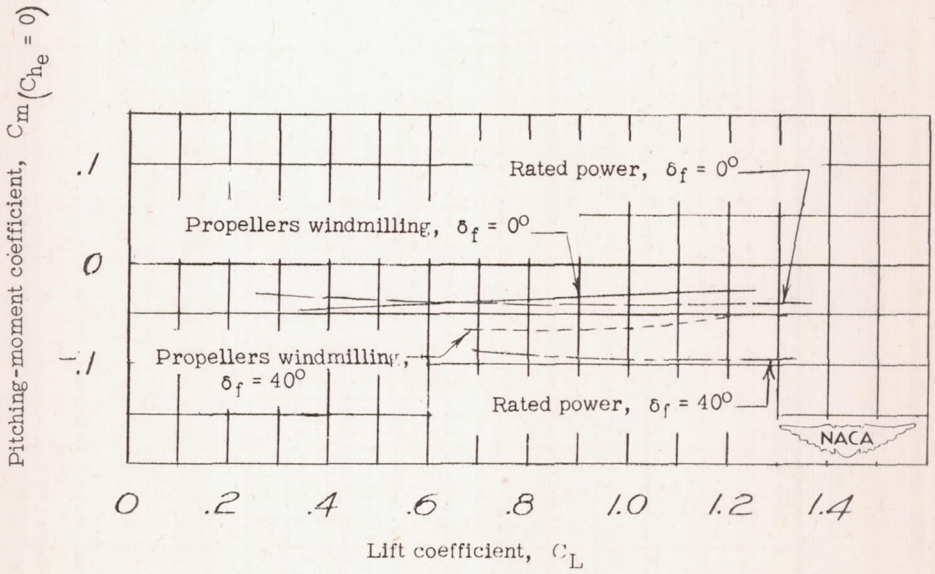

Figure 7.- Effect of power and flap deflection on the variation of C_m with C_L. Stick free; center of gravity at 0.23 mean aerodynamic chord; $i_t = 1.4^\circ$; $\delta_a = 0^\circ$; $\delta_r = 0^\circ$.

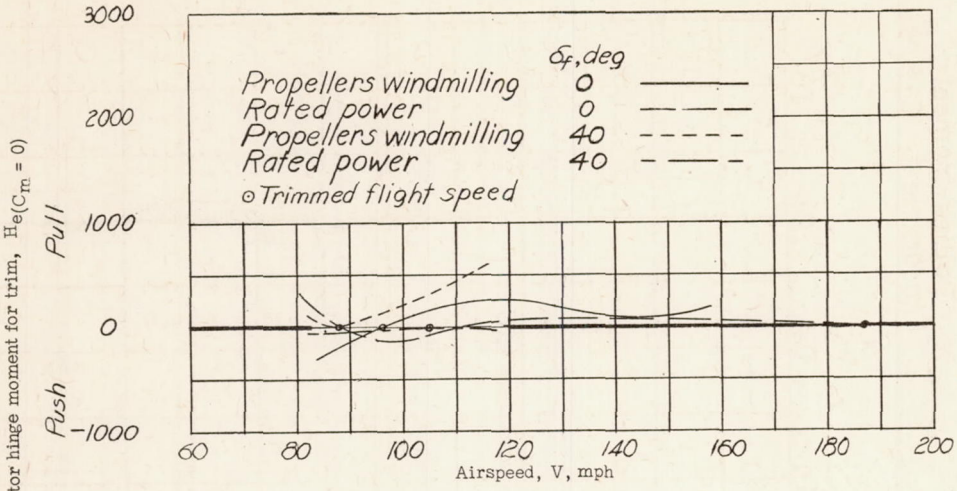

(a) Assumed trimmed flight conditions.

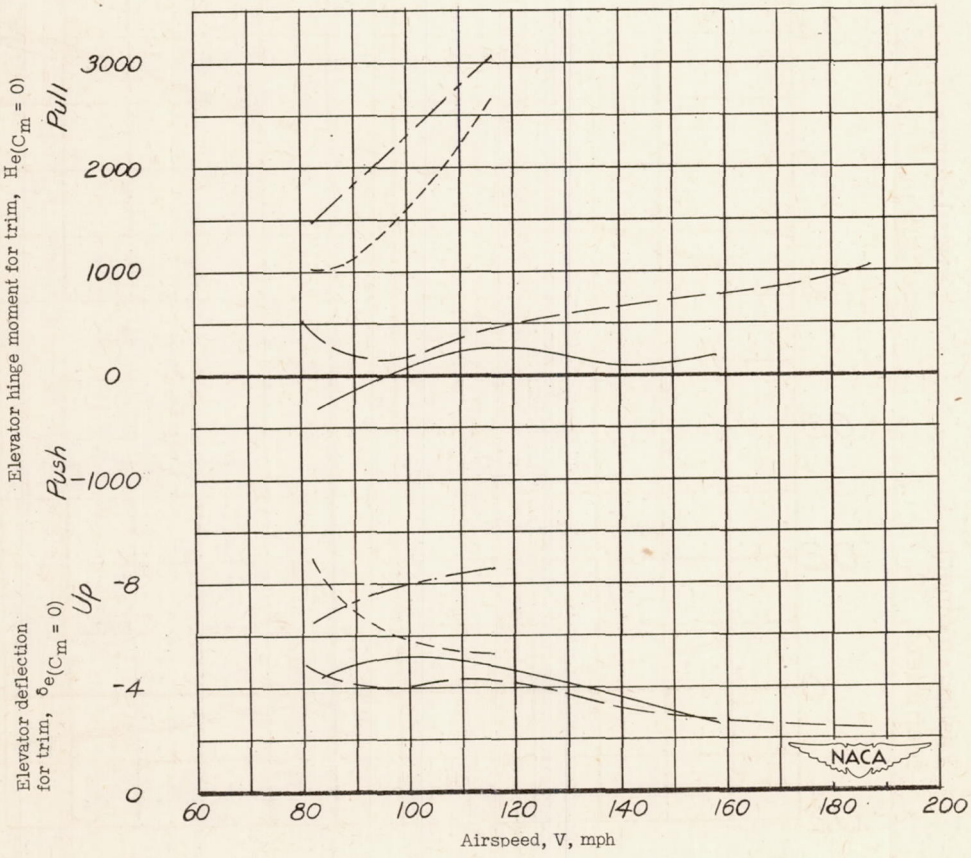

(b) Tab neutral test conditions.

Figure 8.- Variation of elevator deflection and elevator hinge moment for trim with airspeed at sea level. Center of gravity at 0.23 mean aerodynamic chord; $i_t = 1.4^{\circ}$; $\delta_a = 0^{\circ}$; $\delta_r = 0^{\circ}$.

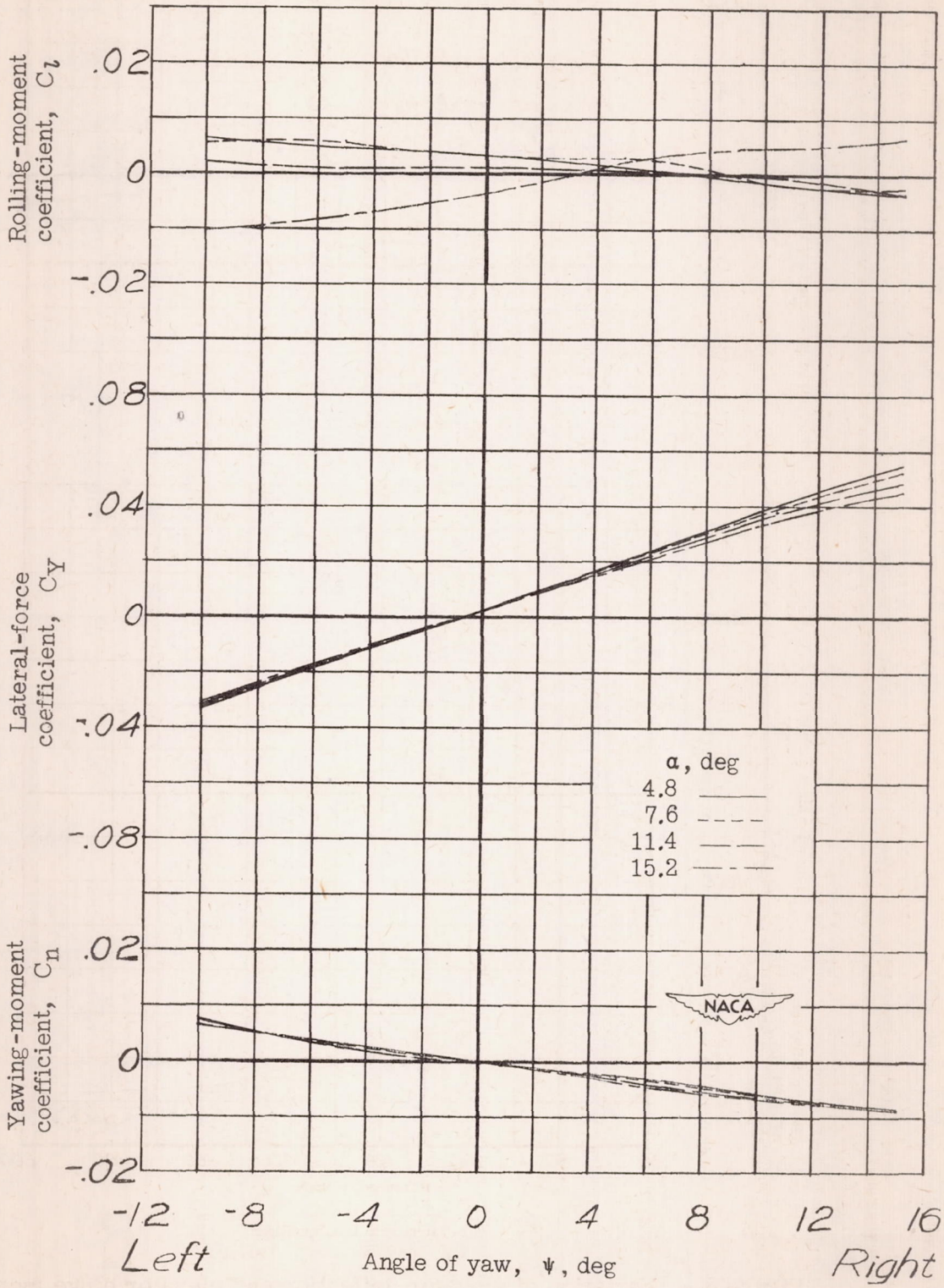

(a) Propellers windmilling; $\delta_f = 40^{\circ}$.

Figure 9.- Variation of C_n, C_Y, and C_l with ψ. Controls neutral.

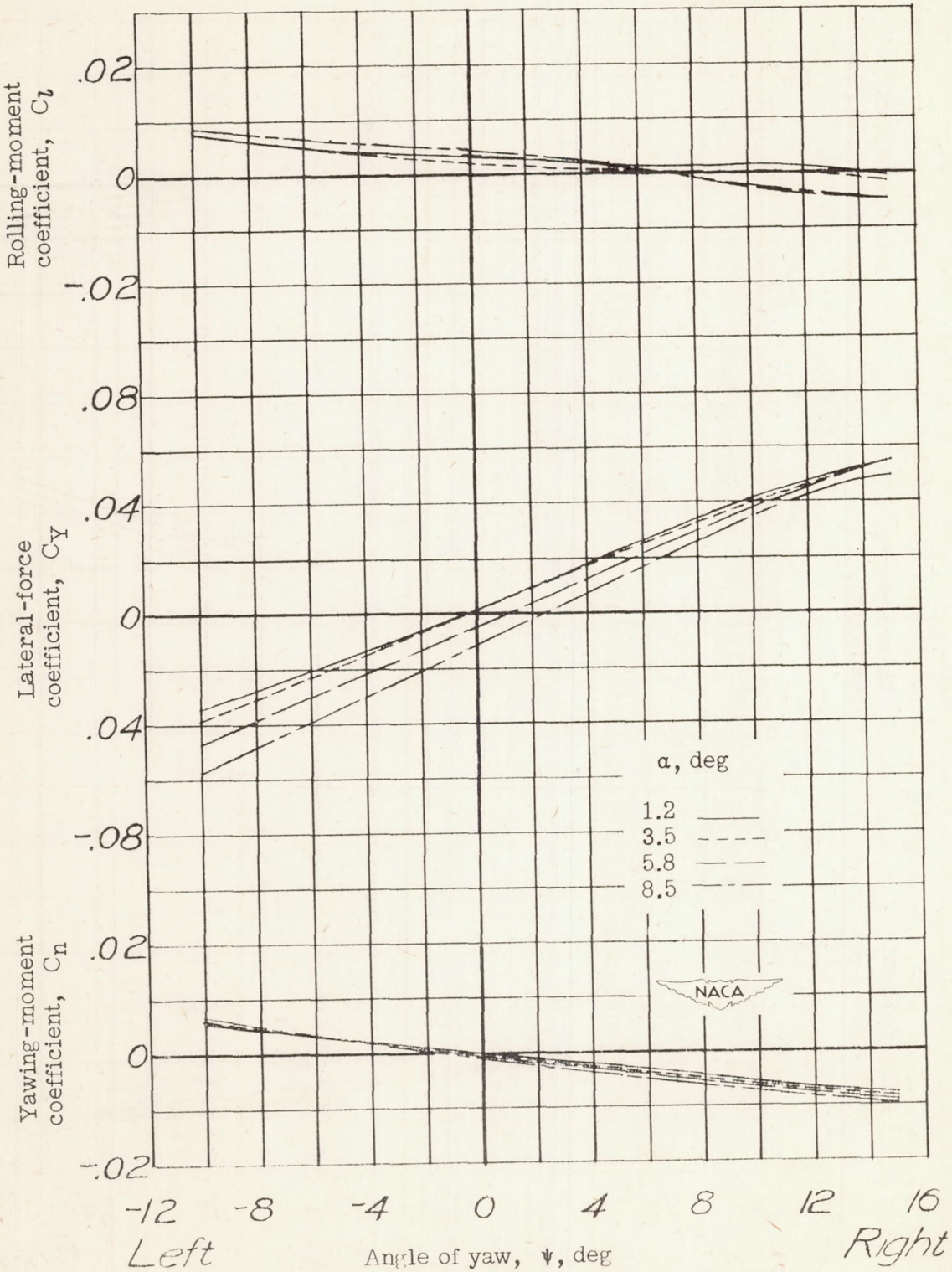

(b) Rated power; $\delta_f = 0^{\circ}$.

Figure 9.- Continued.

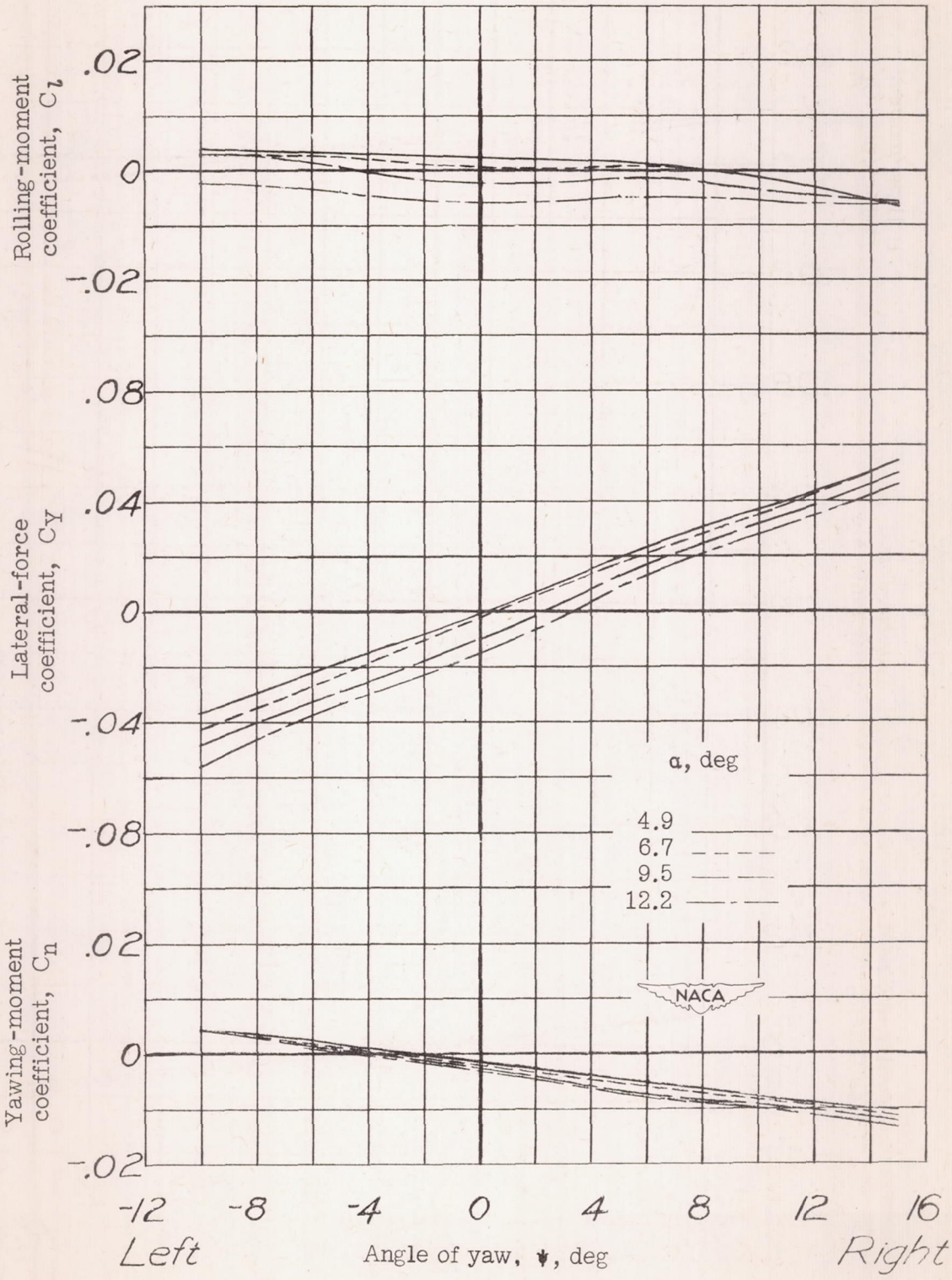

(c) Asymmetric power; $\delta_f = 0^{\circ}$.

Figure 9.- Concluded.

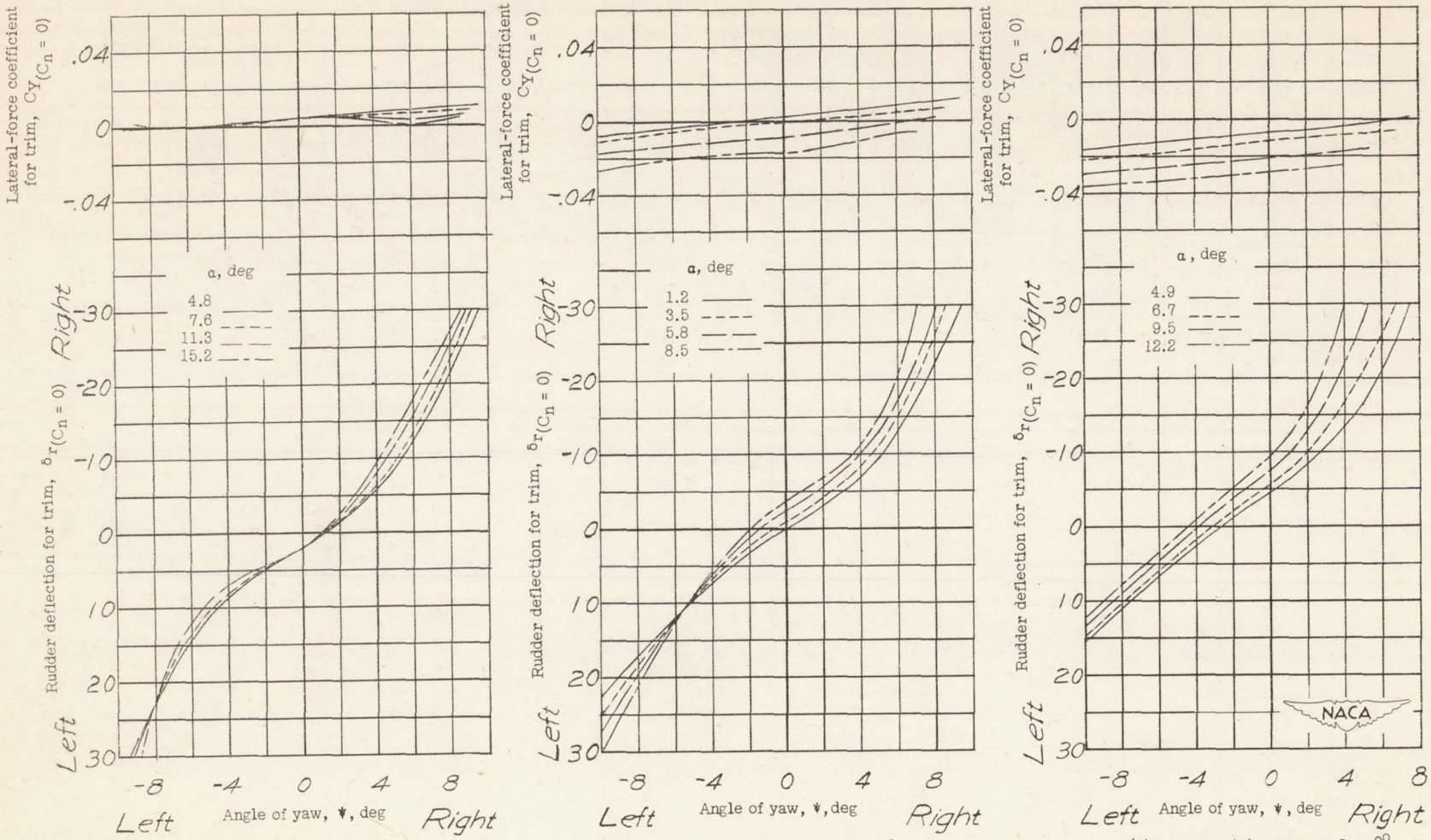

(a) Propellers windmilling; $\delta_f = 40^\circ$.

(b) Rated power; $\delta_f = 0^\circ$.

(c) Asymmetric power; $\delta_f = 0^\circ$.

Figure 10.- Variation of rudder deflection and lateral-force coefficient for trim with angle of yaw. $\delta_a = 0^\circ$; $\delta_e = 0^\circ$.

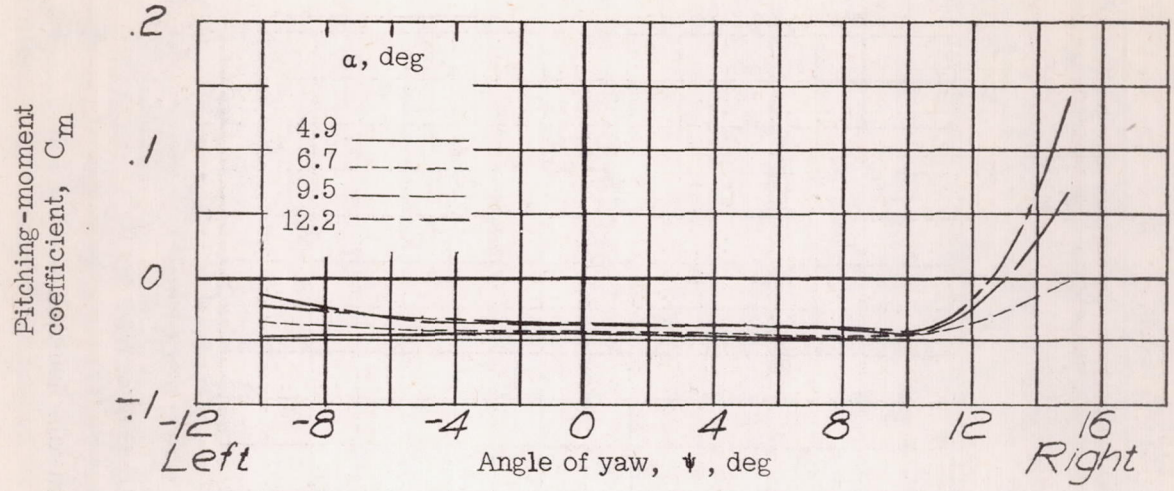

(a) Asymmetric power; $\delta_f = 0^{\circ}$.

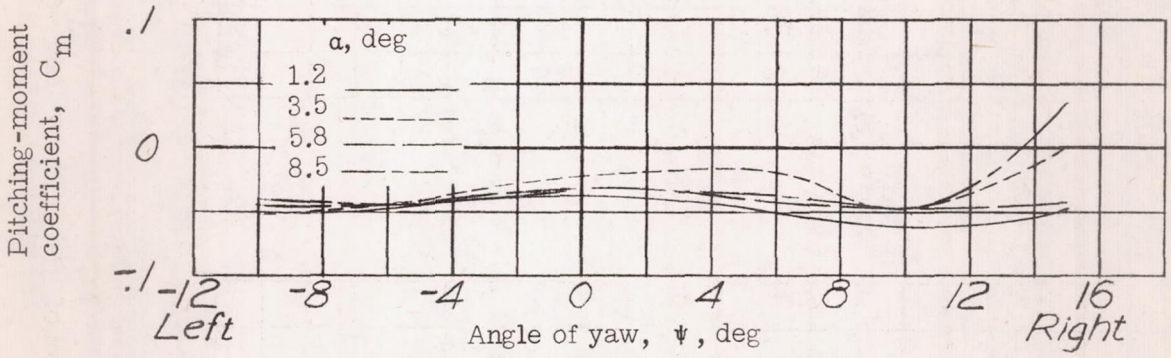

(b) Rated power; $\delta_f = 0^{\circ}$.

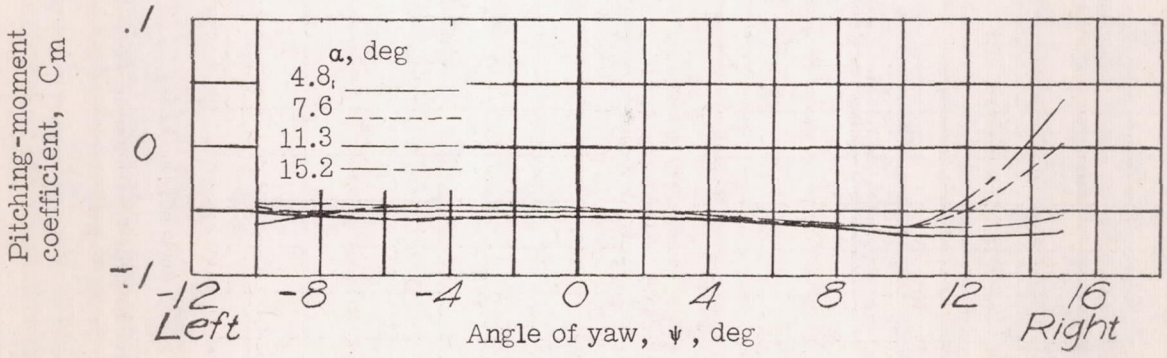

(c) Propellers windmilling; $\delta_f = 40^{\circ}$.

Figure 11.- Variation of C_m with ψ and α. Controls neutral; center of gravity at 0.25 mean aerodynamic chord.

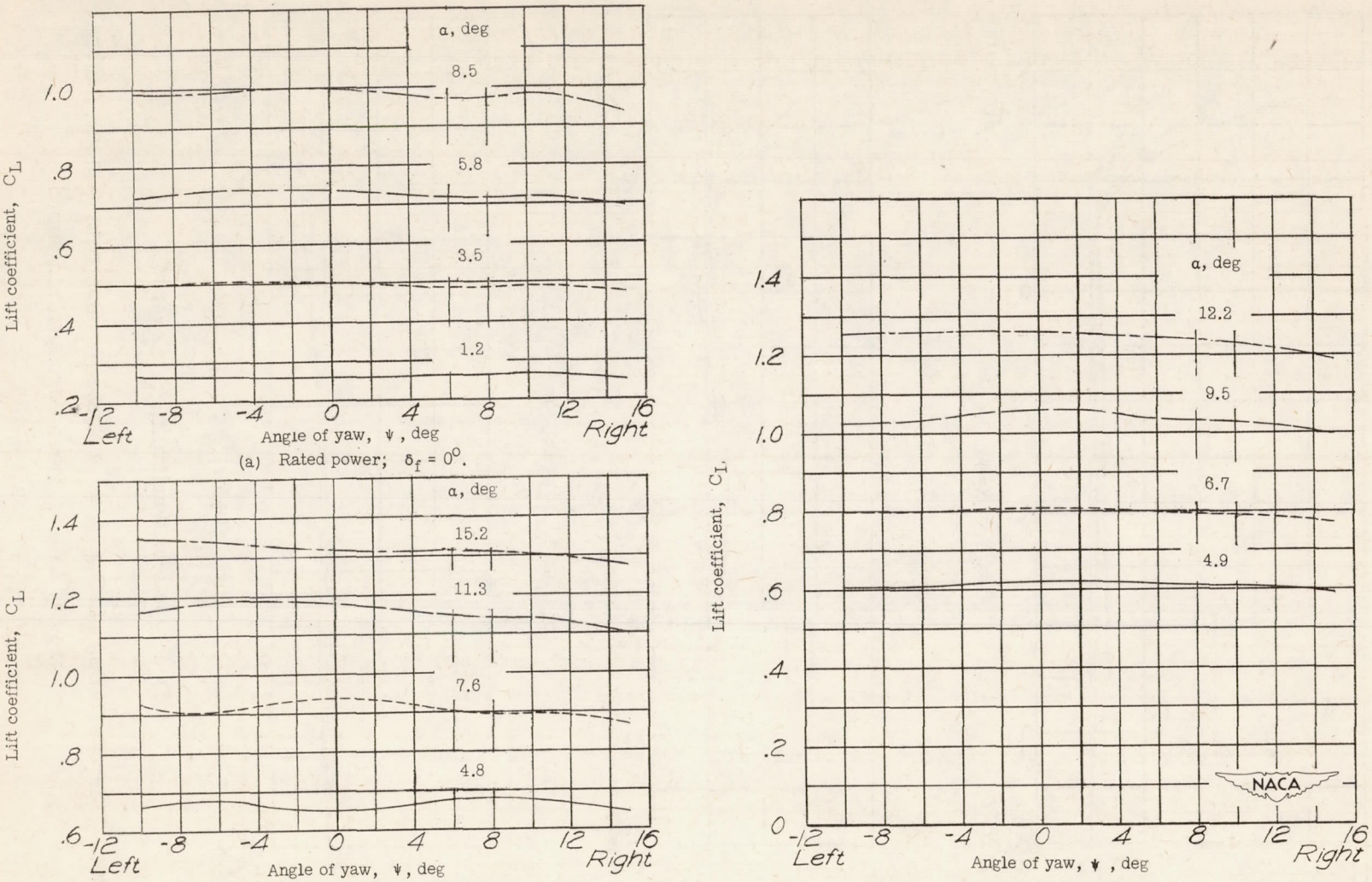

(a) Rated power; $\delta_f = 0^\circ$.

(b) Propellers windmilling; $\delta_f = 40^\circ$.

(c) Asymmetric power; $\delta_f = 0^\circ$.

Figure 12.- Variation of C_L with ψ and α. Controls neutral.

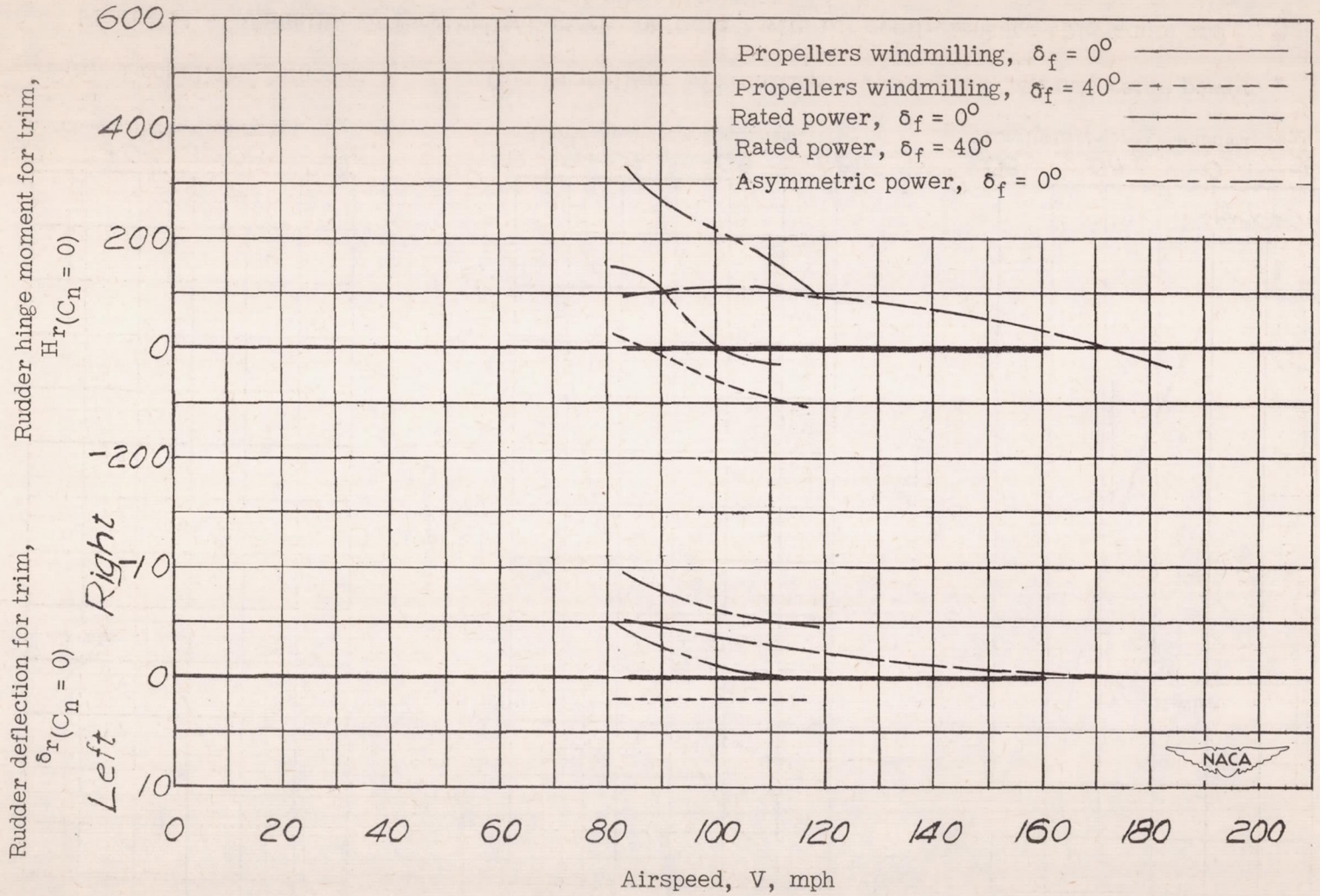

Figure 13.- Effect of power and flap deflection on the variation of rudder deflection and rudder hinge moment for trim with airspeed. Sea level; $\psi = 0^\circ$; $\delta_a = 0^\circ$; $\delta_e = 0^\circ$.

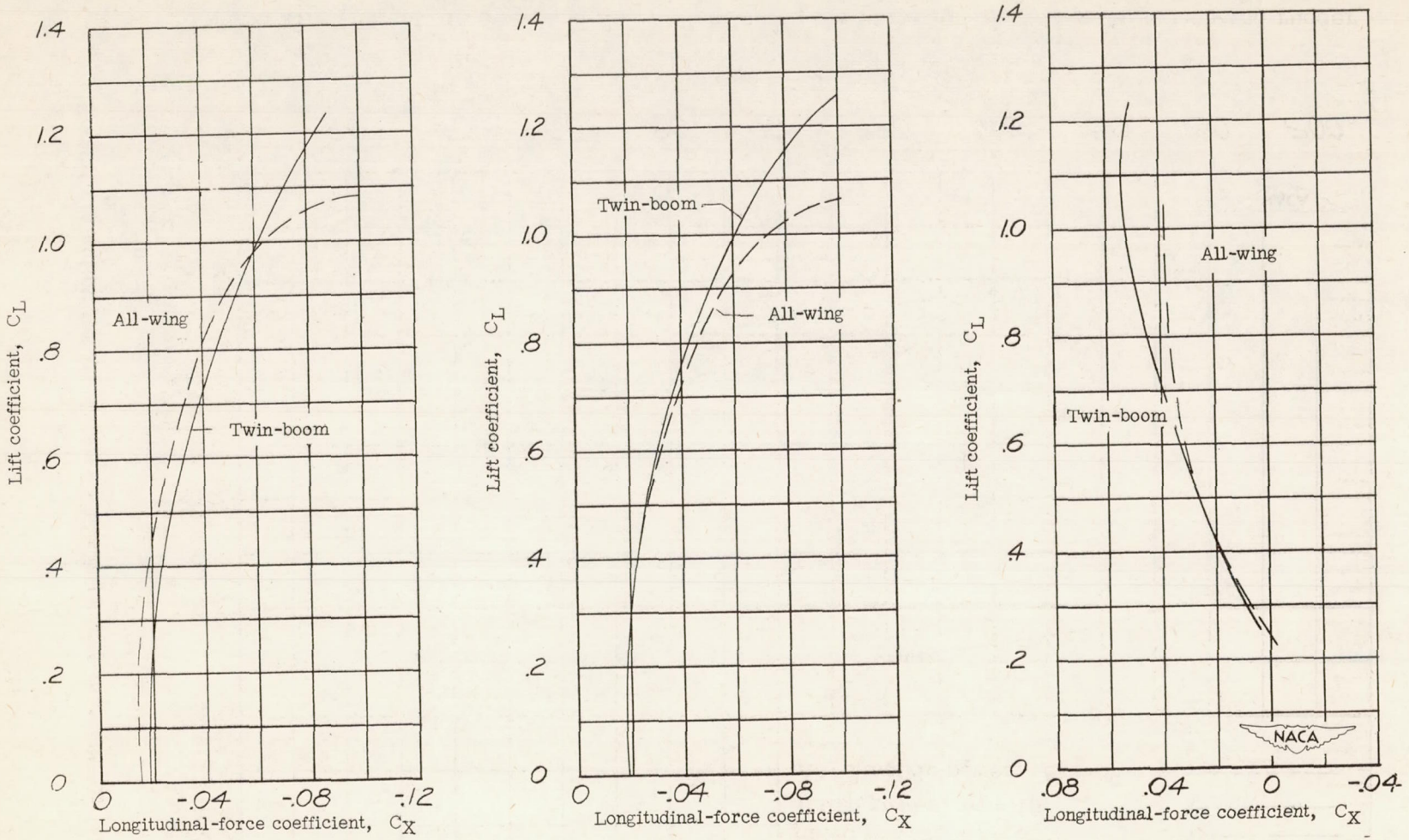

(a) Propellers removed. (b) Propellers windmilling. (c) Normal rated power.

Figure 14.- Variation of longitudinal-force coefficient with lift coefficient for twin-boom and all-wing airplanes.

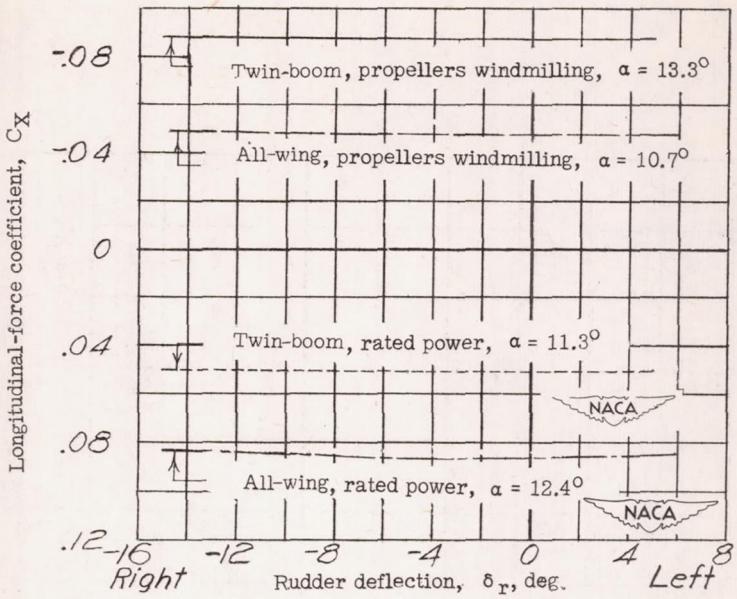

Figure 15.- Variation of longitudinal-force coefficient with rudder deflection for the twin-boom and the all-wing airplanes at high angles of attack. Propellers windmilling; rated power; $\delta_a = 0^\circ$; $\delta_e = 0^\circ$; $\delta_f = 0^\circ$.

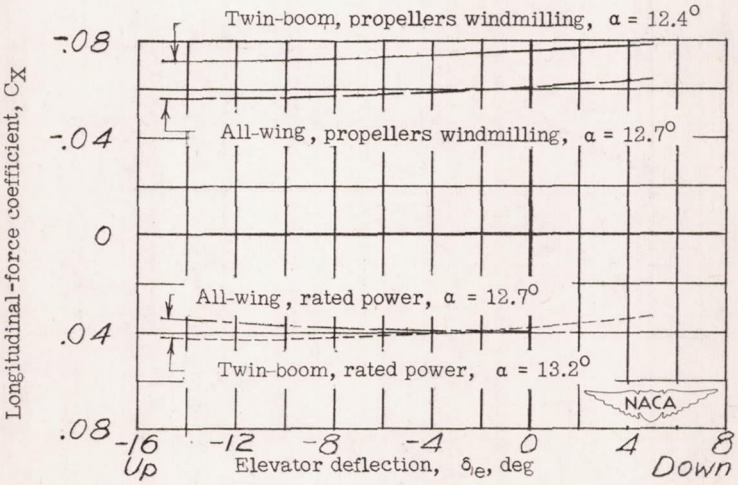

Figure 16.- Variation of longitudinal-force coefficient with elevator deflection for the twin-boom and the all-wing airplanes at high angles of attack. Propellers windmilling; rated power; $\delta_a = 0^\circ$; $\delta_f = 0^\circ$; $\delta_r = 0^\circ$.

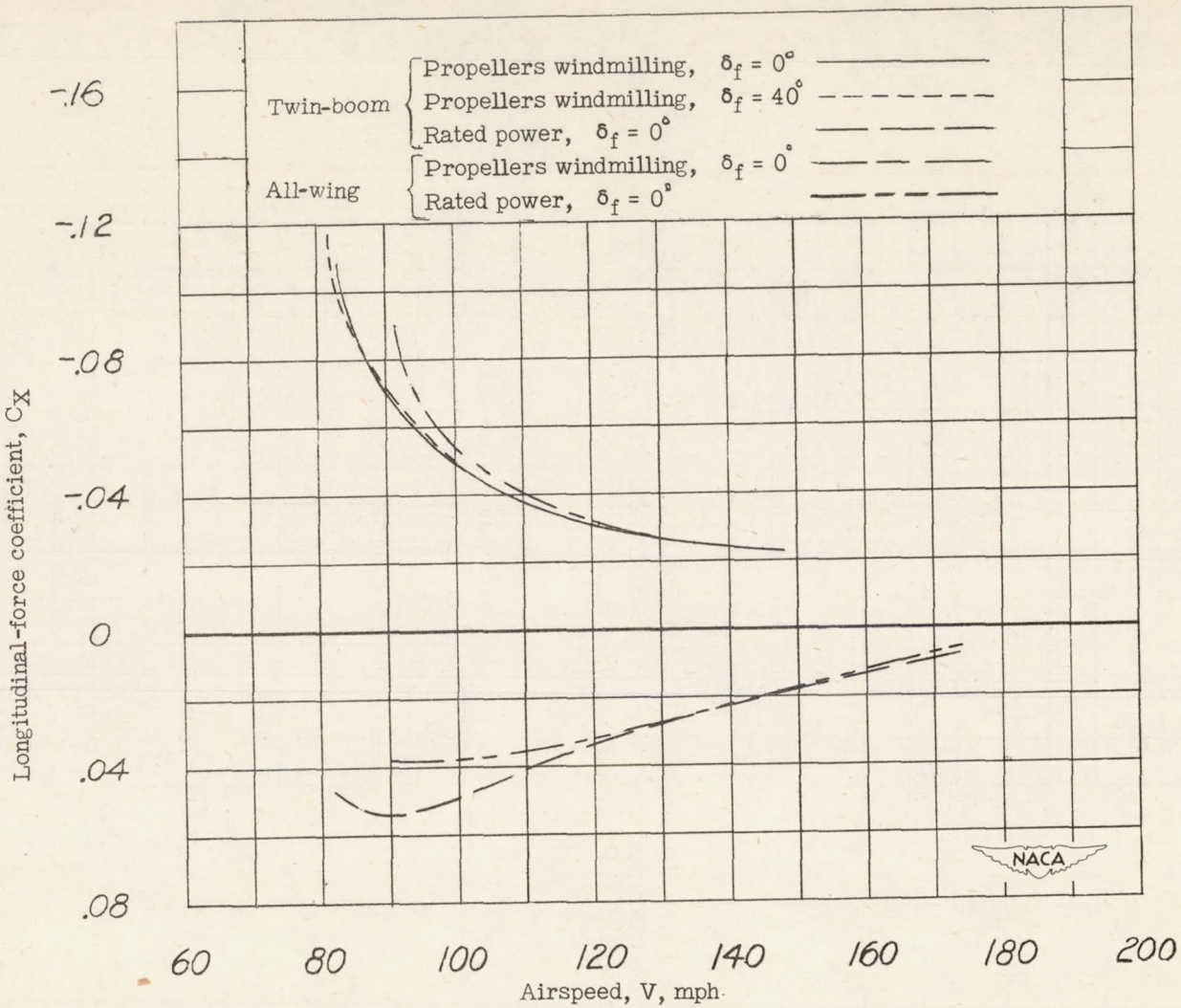

Figure 17.- Variation of longitudinal-force coefficient with airspeed at sea level for twin-boom and all-wing airplanes. Controls neutral.

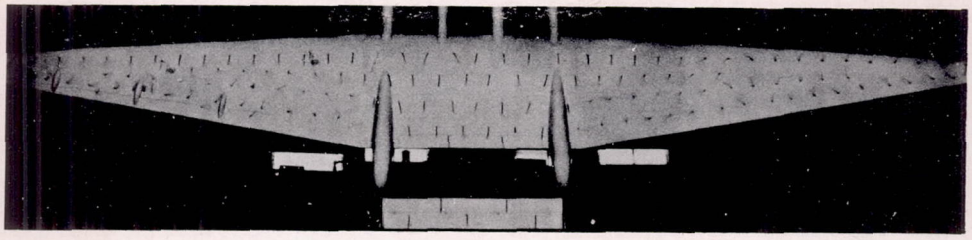

$\alpha = 16.9^{\circ}$; $C_L = 1.28$

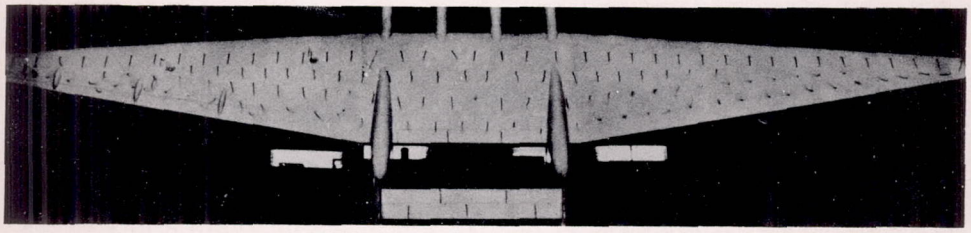

$\alpha = 14.1^{\circ}$; $C_L = 1.24$

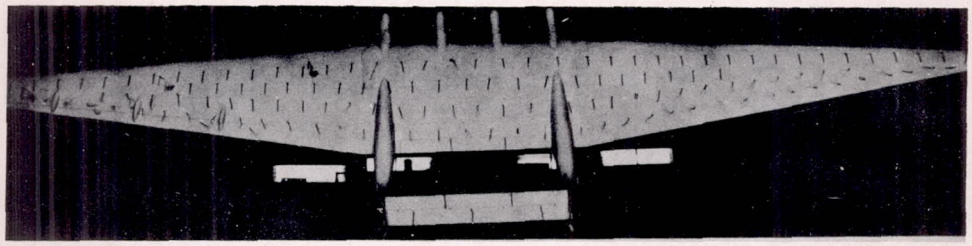

$\alpha = 12.3^{\circ}$; $C_L = 1.15$

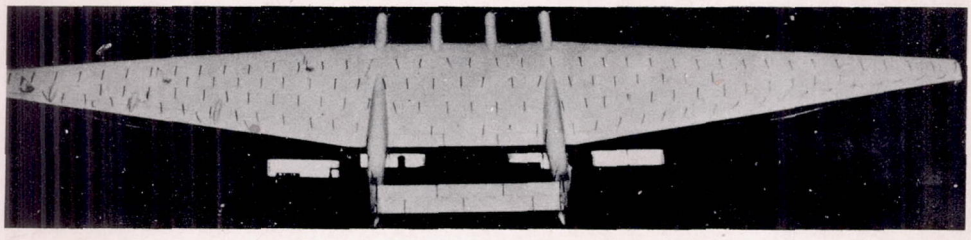

$\alpha = 9.5^{\circ}$; $C_L = 0.96$

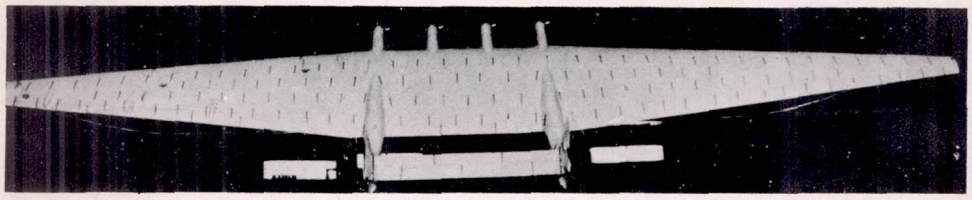

$\alpha = -0.5^{\circ}$; $C_L = 0$

NACA
L-57087

Figure 18.- Stall progression over the $\frac{1}{7}$-scale model of the twin-boom airplane. Propellers windmilling; controls neutral; $V \approx 55$ miles per hour.

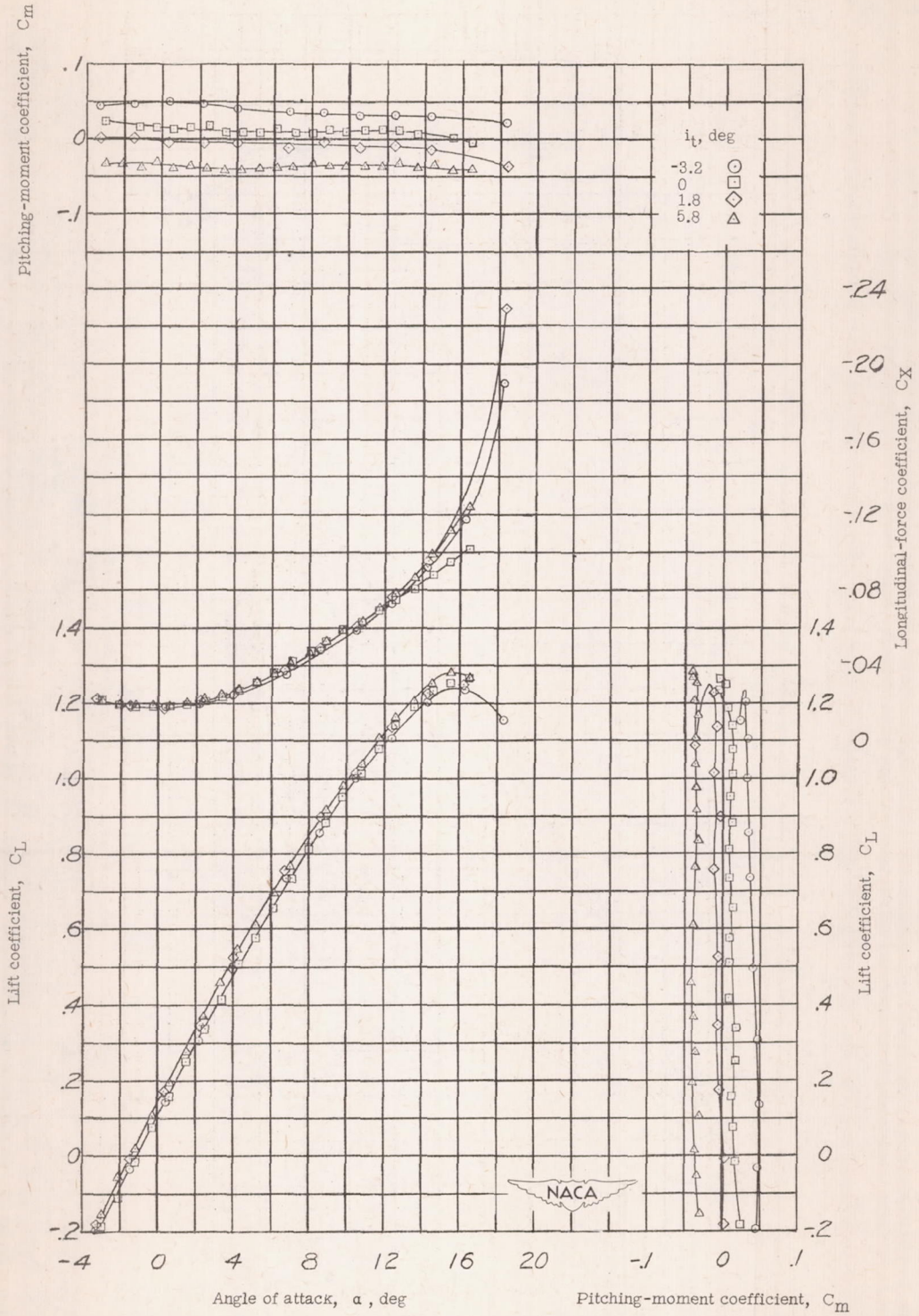

Figure 19.- Effect of horizontal-stabilizer setting on the variation of C_L, C_X, and C_m with α. Propellers removed; $\psi = 0^{\circ}$; controls neutral.

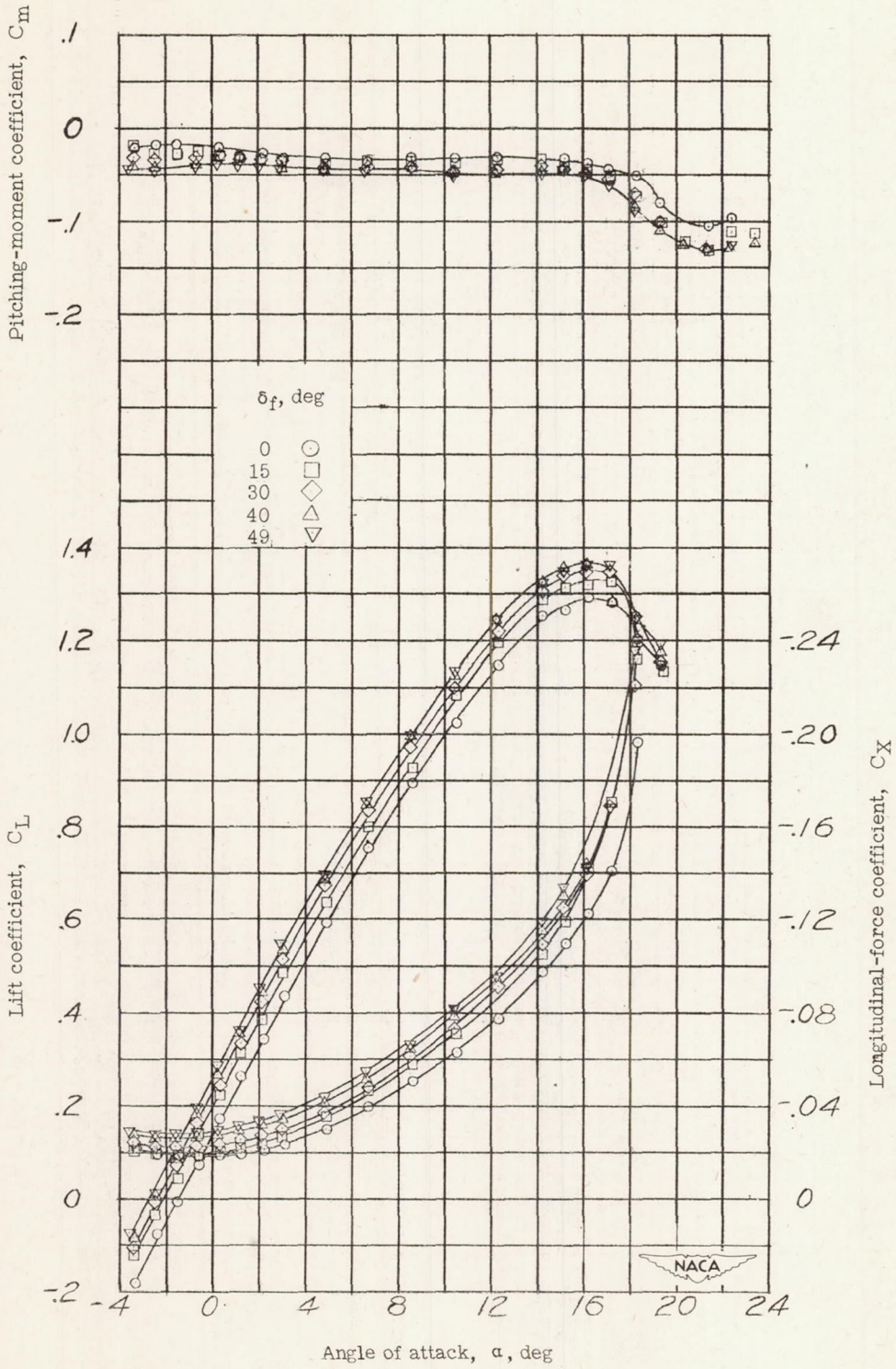

Figure 20.- Effect of flap deflection on the variation of C_L, C_X, and C_m with α. Propellers windmilling; $\psi = 0^{\circ}$; $i_t = 5.4^{\circ}$; controls neutral.

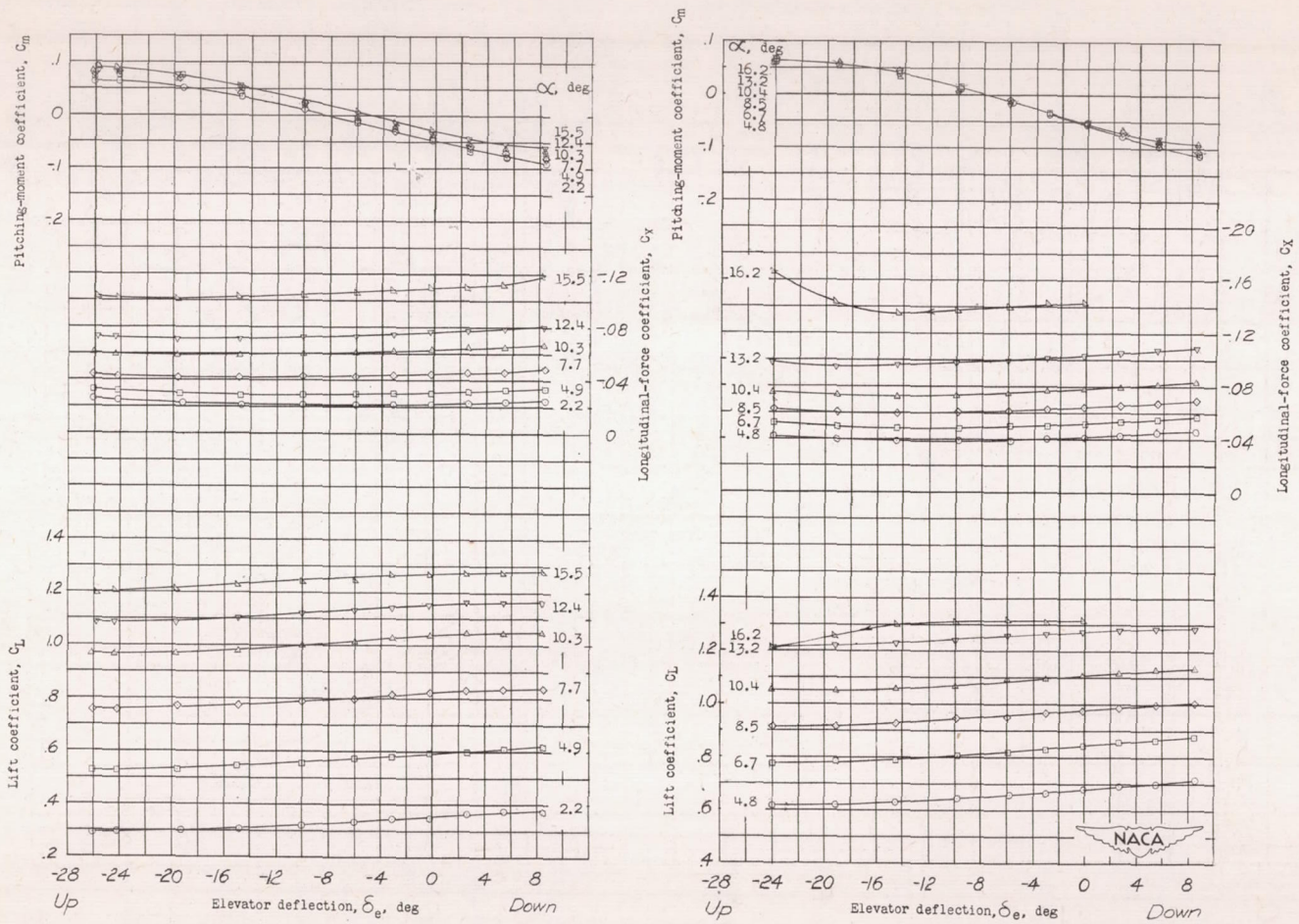

(a) $\delta_f = 0^\circ$.

(b) $\delta_f = 40^\circ$.

Figure 21.- Effect of α and δ_f on the variation of C_L, C_X, and C_m with δ_e. Propellers windmilling; $\psi = 0^\circ$; $i_t = 5.4^\circ$; $\delta_a = 0^\circ$; $\delta_r = 0^\circ$.

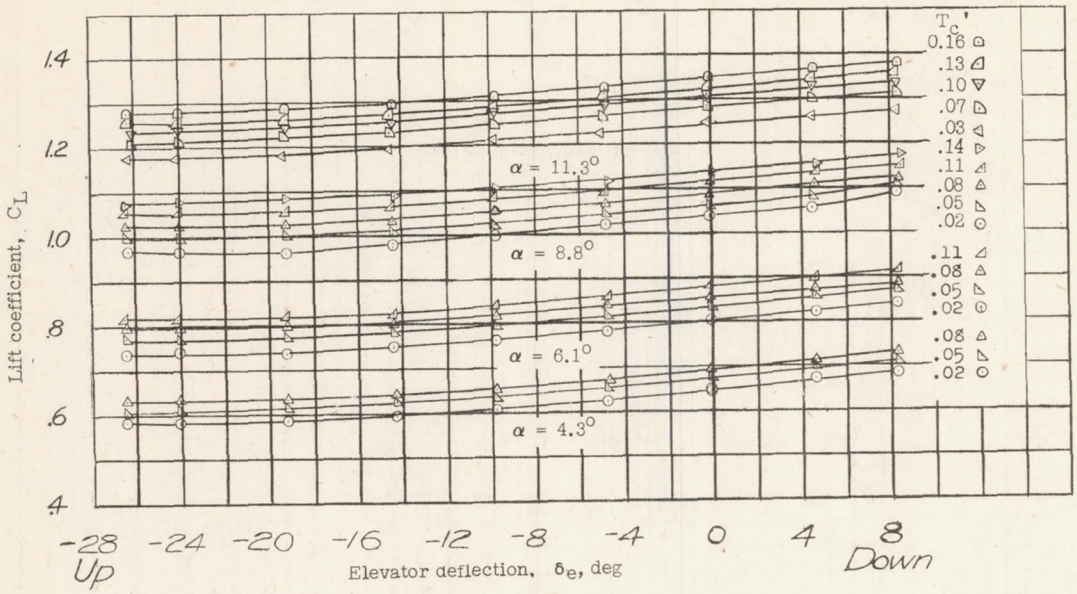

(a) $\delta_f = 40^\circ$.

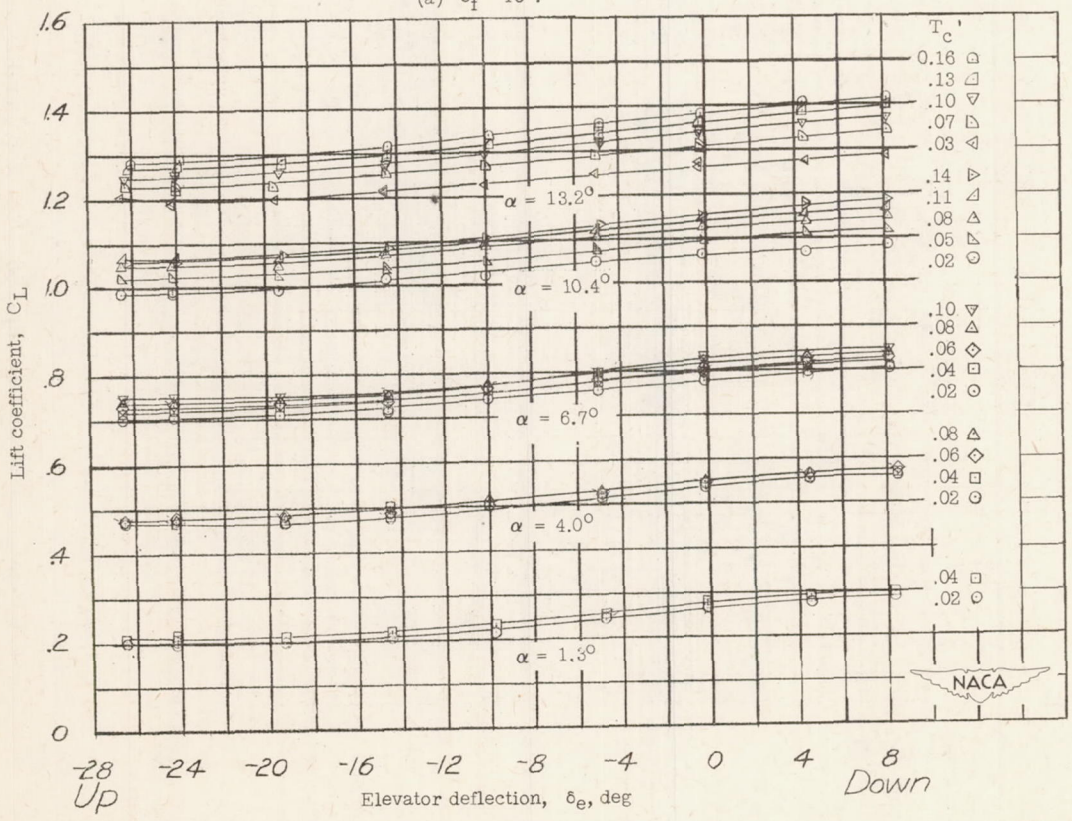

(b) $\delta_f = 0^\circ$.

Figure 22.- Effect of α and T_c' on the variation of C_L with δ_e. $\psi = 0^\circ$; $i_t = 5.4^\circ$; $\delta_a = 0^\circ$; $\delta_r = 0^\circ$.

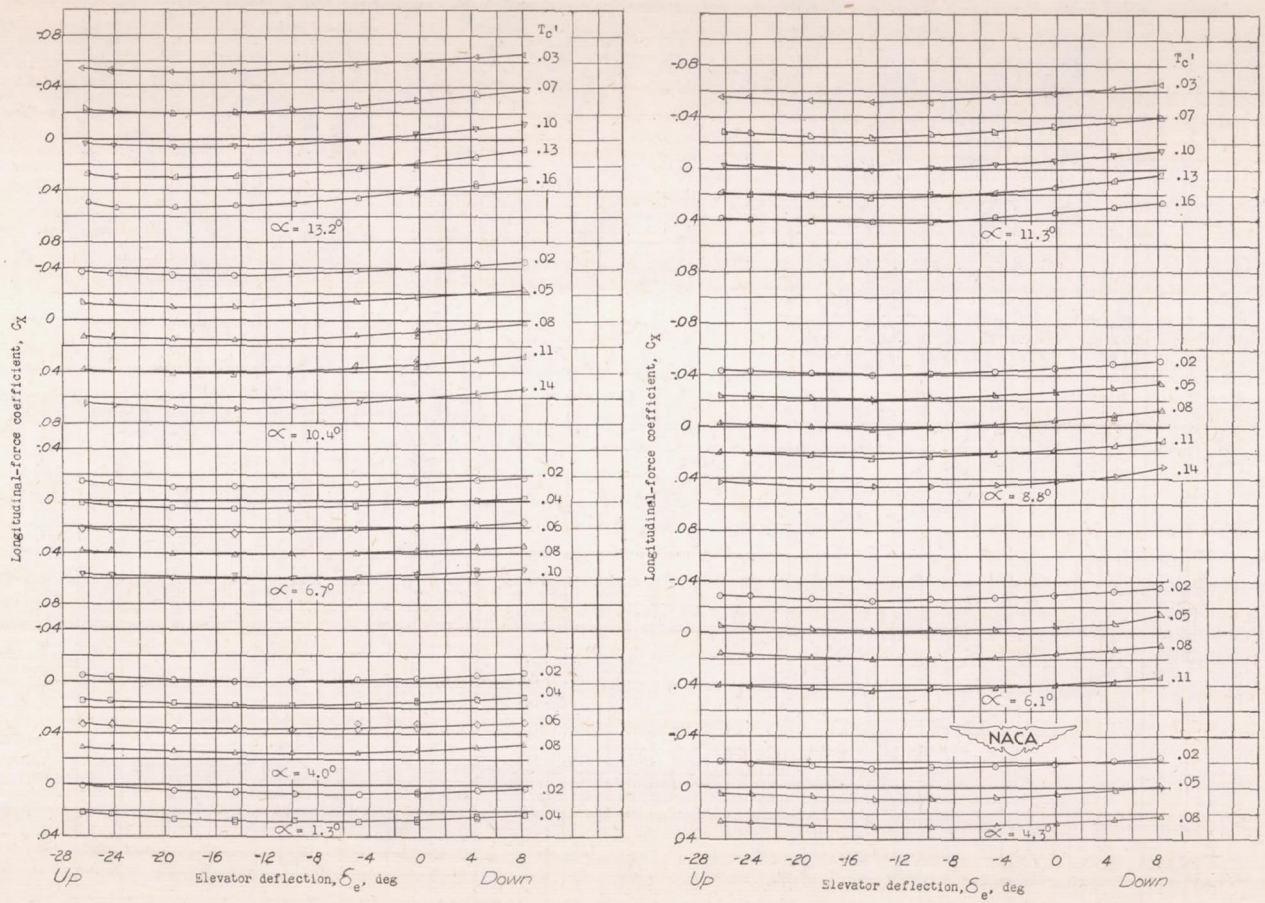

(a) $\delta_f = 0^\circ$.

(b) $\delta_f = 40^\circ$.

Figure 23.- Effect of α, T_c', and δ_f on the variation of C_X with δ_e.
$\psi = 0^\circ$; $i_t = 5.4^\circ$; $\delta_a = 0^\circ$; $\delta_r = 0^\circ$.

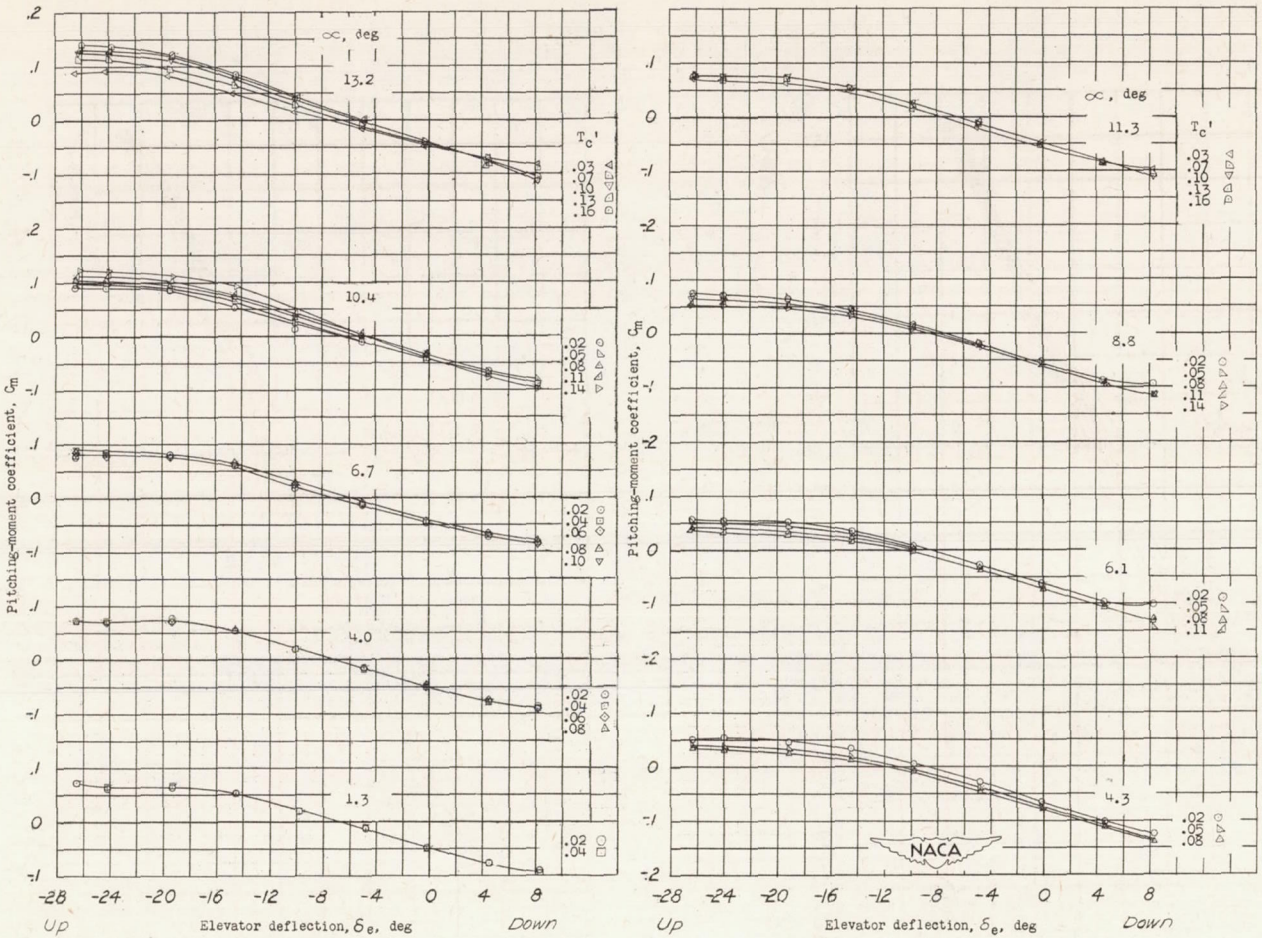

(a) $\delta_f = 0^{\circ}$.

(b) $\delta_f = 40^{\circ}$.

Figure 24.- Effect of α, T_c', and δ_f on the variation of C_m with δ_e. $\psi = 0^{\circ}$; $i_t = 5.4^{\circ}$; $\delta_a = 0^{\circ}$; $\delta_r = 0^{\circ}$.

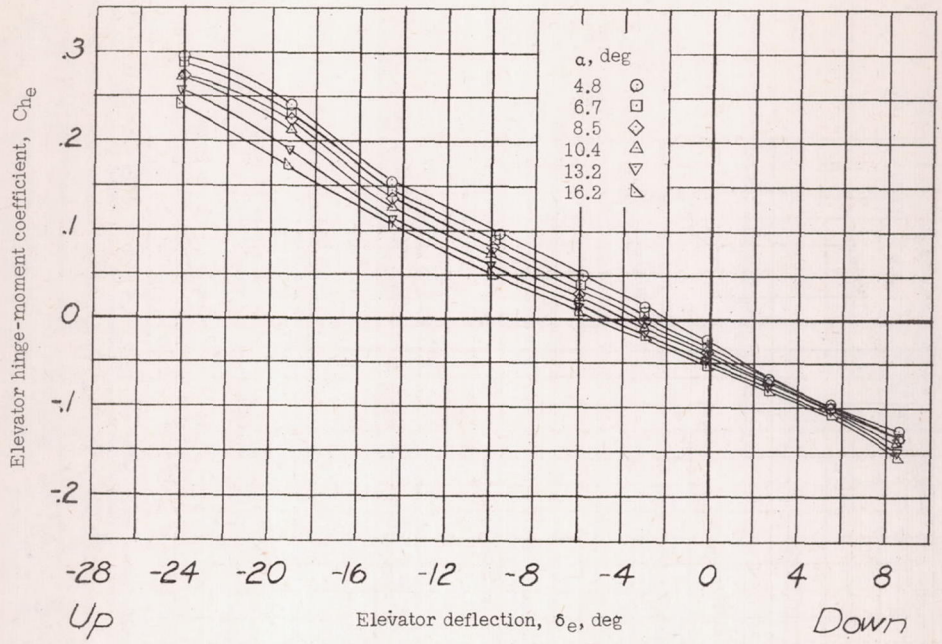

(a) $\delta_f = 40^{\circ}$.

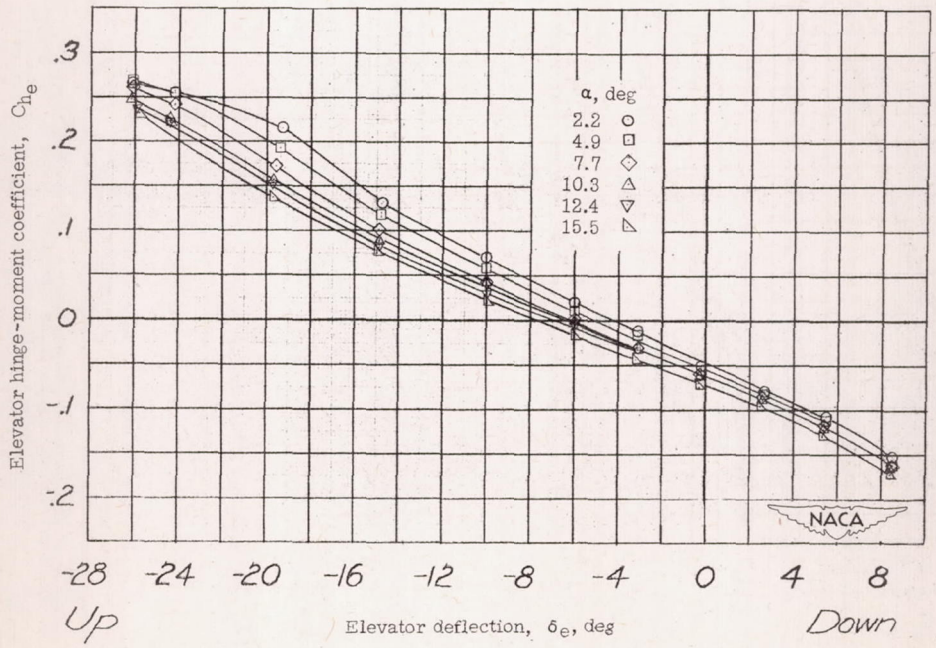

(b) $\delta_f = 0^{\circ}$.

Figure 25.- Effect of α and δ_f on the variation of C_{h_e} with δ_e. Propellers windmilling; $\psi = 0^{\circ}$; $i_t = 5.4^{\circ}$; $\delta_a = 0^{\circ}$; $\delta_r = 0^{\circ}$.

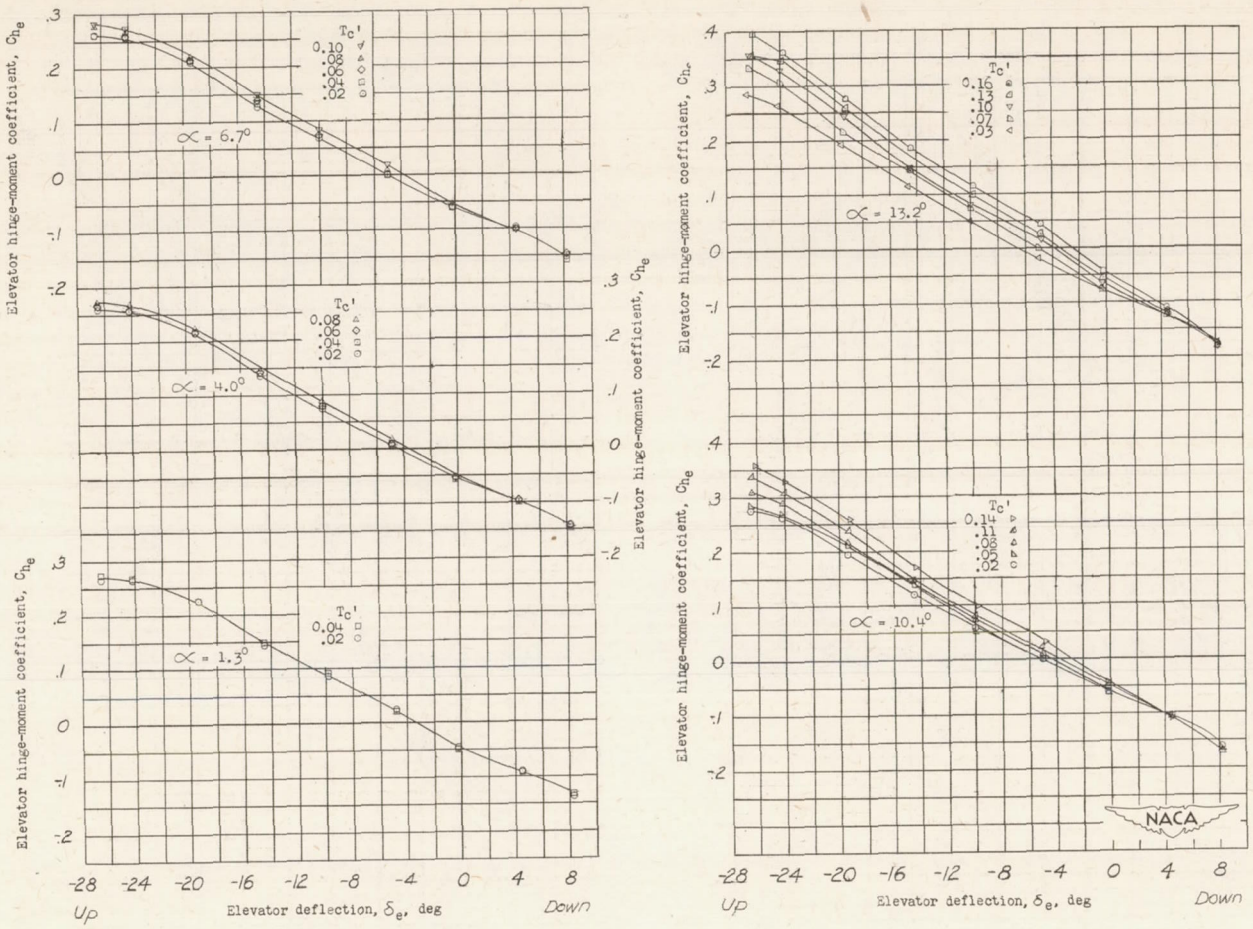

(a) $\delta_f = 0^\circ$.

Figure 26.- Effect of α, T_c', and δ_f on the variation of C_{h_e} with δ_e. $\psi = 0^\circ$; $i_t = 5.4^\circ$; $\delta_a = 0^\circ$; $\delta_r = 0^\circ$.

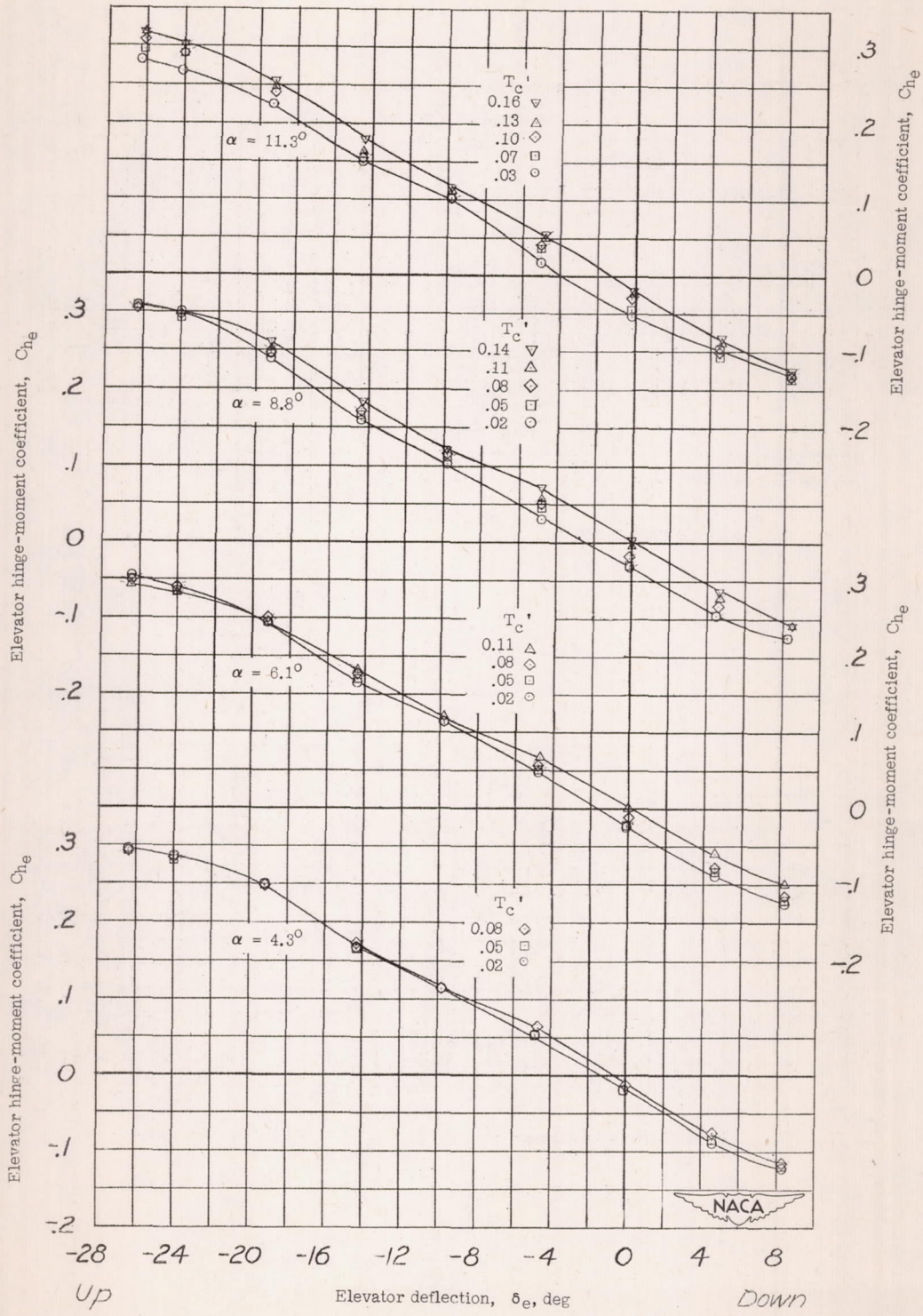

(b) $\delta_f = 40^\circ$.

Figure 26.- Concluded.

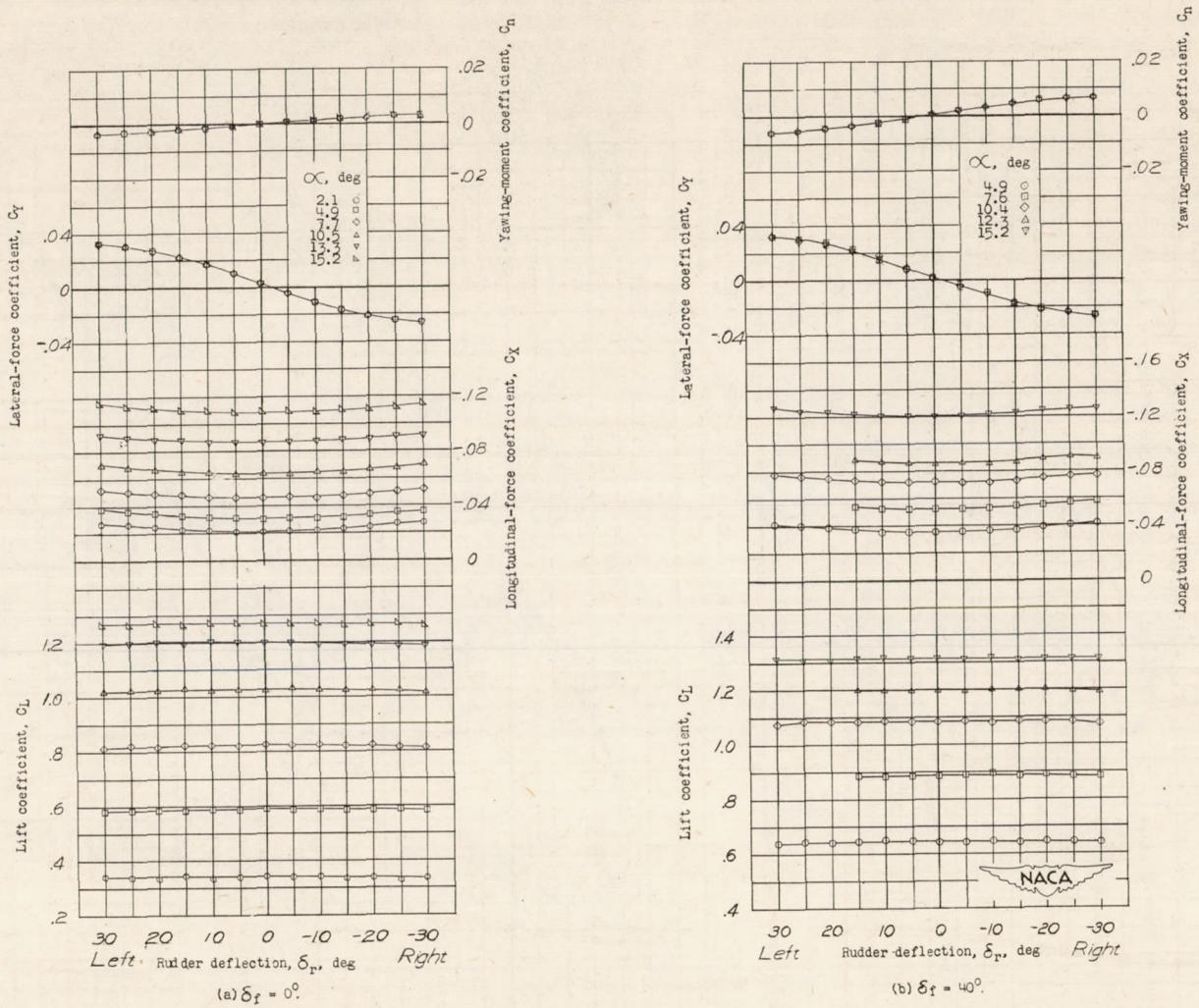

Figure 27.- Effect of α and δ_f on the variation of C_L, C_X, C_Y, and C_n with δ_r. Propellers windmilling; $\psi = 0^\circ$; $i_t = 5.4^\circ$; $\delta_a = 0^\circ$; $\delta_e = 0^\circ$.

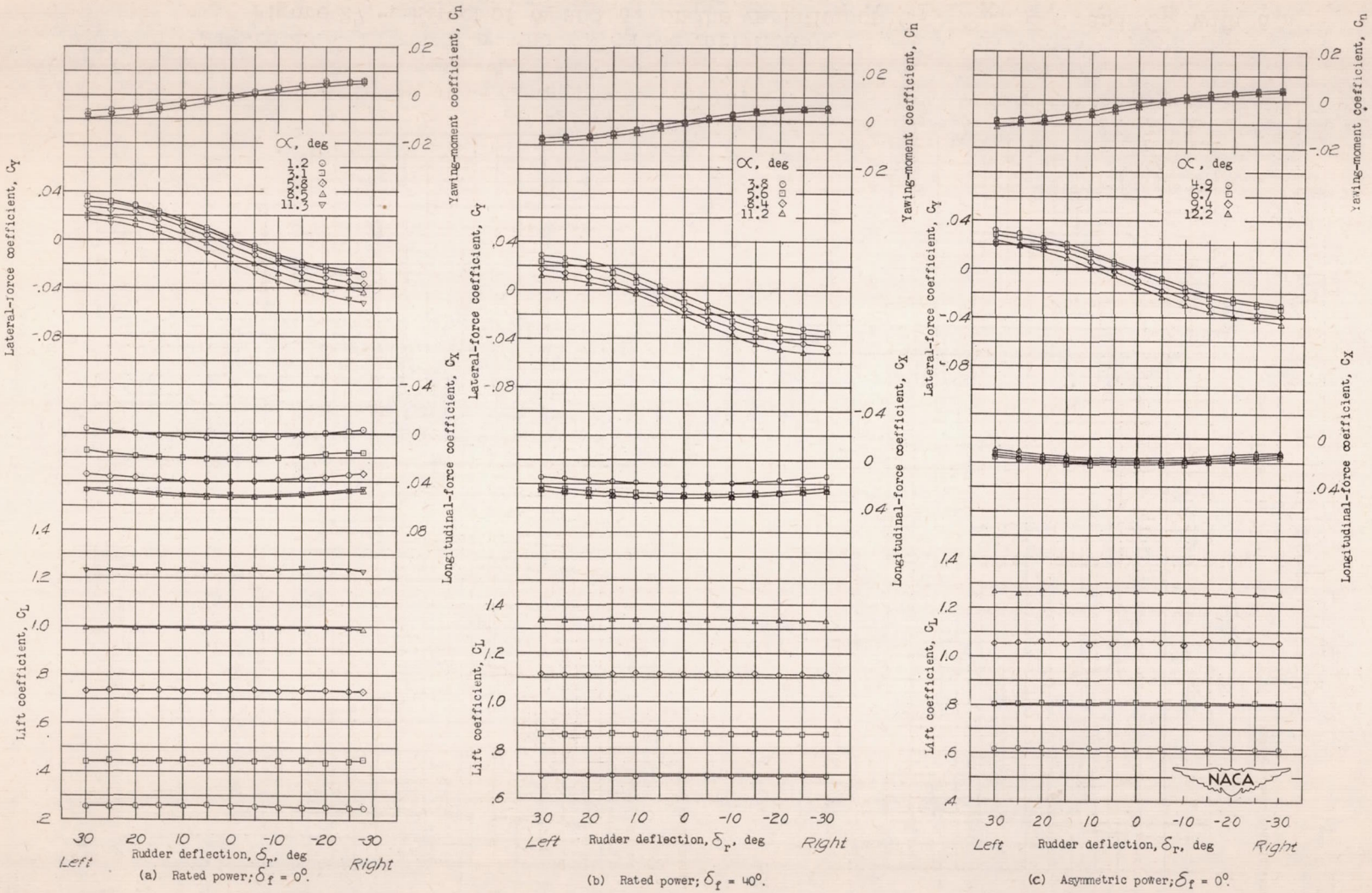

(a) Rated power; $\delta_f = 0^\circ$.

(b) Rated power; $\delta_f = 40^\circ$.

(c) Asymmetric power; $\delta_f = 0^\circ$.

Figure 28.- Effect of angle of attack, power, and flap deflection on the variation of C_L, C_X, C_Y, and C_n with δ_r. $\psi = 0^\circ$; $i_t = 5.4^\circ$; $\delta_a = 0^\circ$; $\delta_e = 0^\circ$.

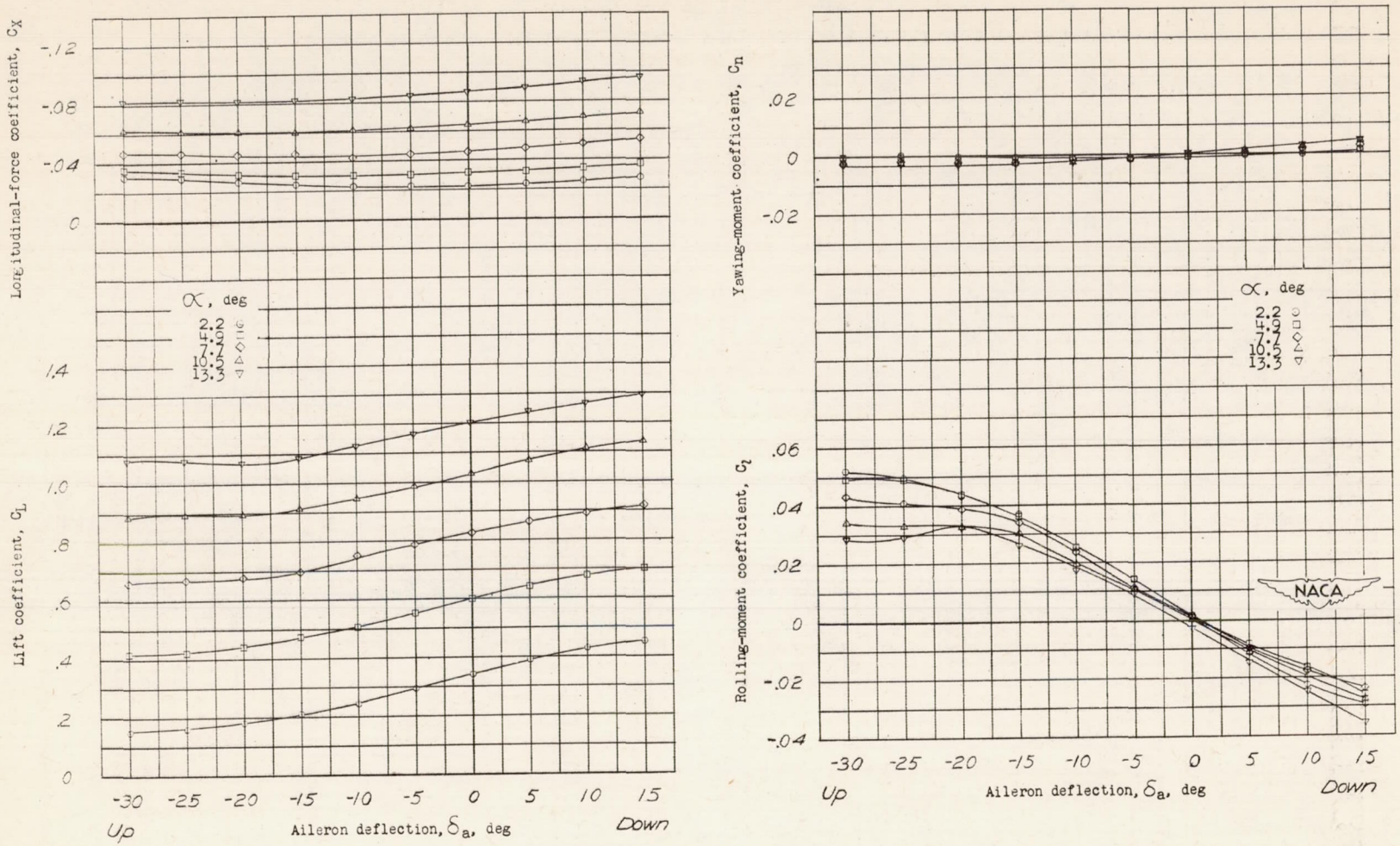

(a) $\delta_f = 0^\circ$.

Figure 29.- Effect of α and δ_f on the variation of C_L, C_X, C_l, and C_n with δ_a. Propellers windmilling; $\psi = 0^\circ$; $i_t = 5.4^\circ$; $\delta_e = 0^\circ$; $\delta_r = 0^\circ$.

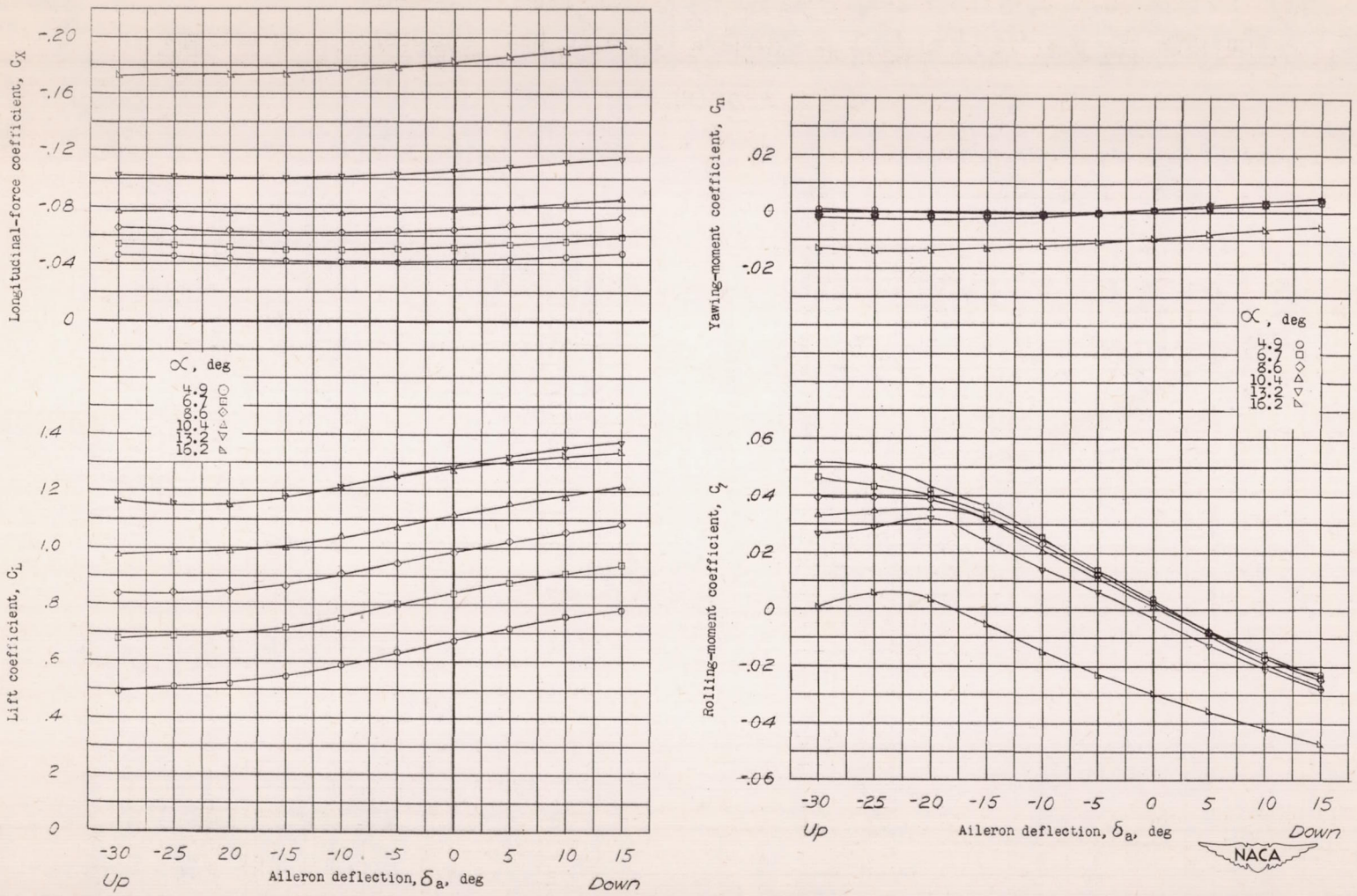

(b) $\delta_f = 40^\circ$.

Figure 29.- Concluded.

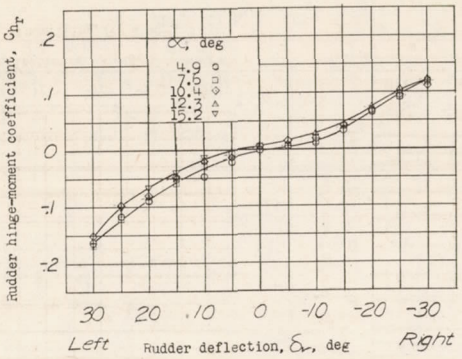

(a) Propellers windmilling; $\delta_f = 40^\circ$.

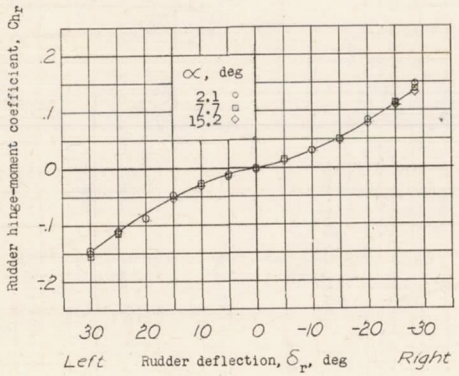

(b) Propellers windmilling; $\delta_f = 0^\circ$.

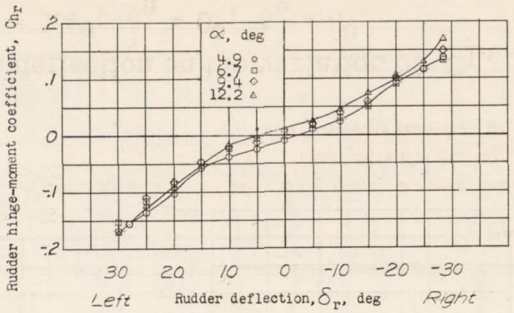

(c) Asymmetric power; $\delta_f = 0^\circ$.

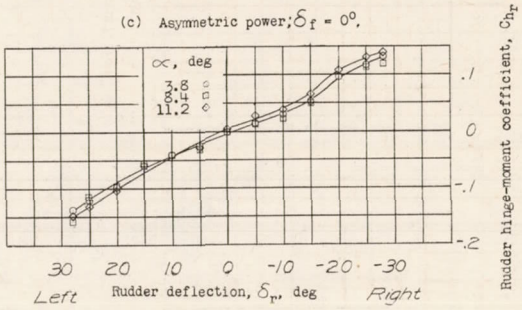

(d) Rated power; $\delta_f = 40^\circ$.

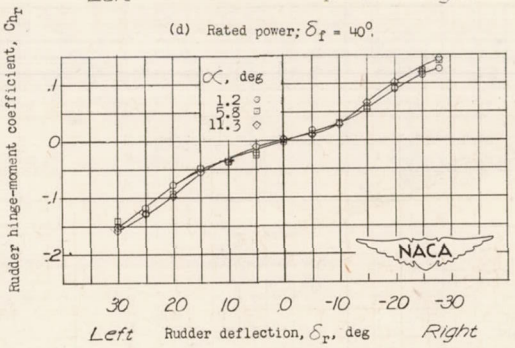

(e) Rated power; $\delta_f = 0^\circ$.

Figure 30.- Effect of angle of attack, power, and flap deflection on the variation of C_{h_r} with δ_r.

$\psi = 0^\circ$; $i_t = 5.4^\circ$; $\delta_a = 0^\circ$; $\delta_e = 0^\circ$.

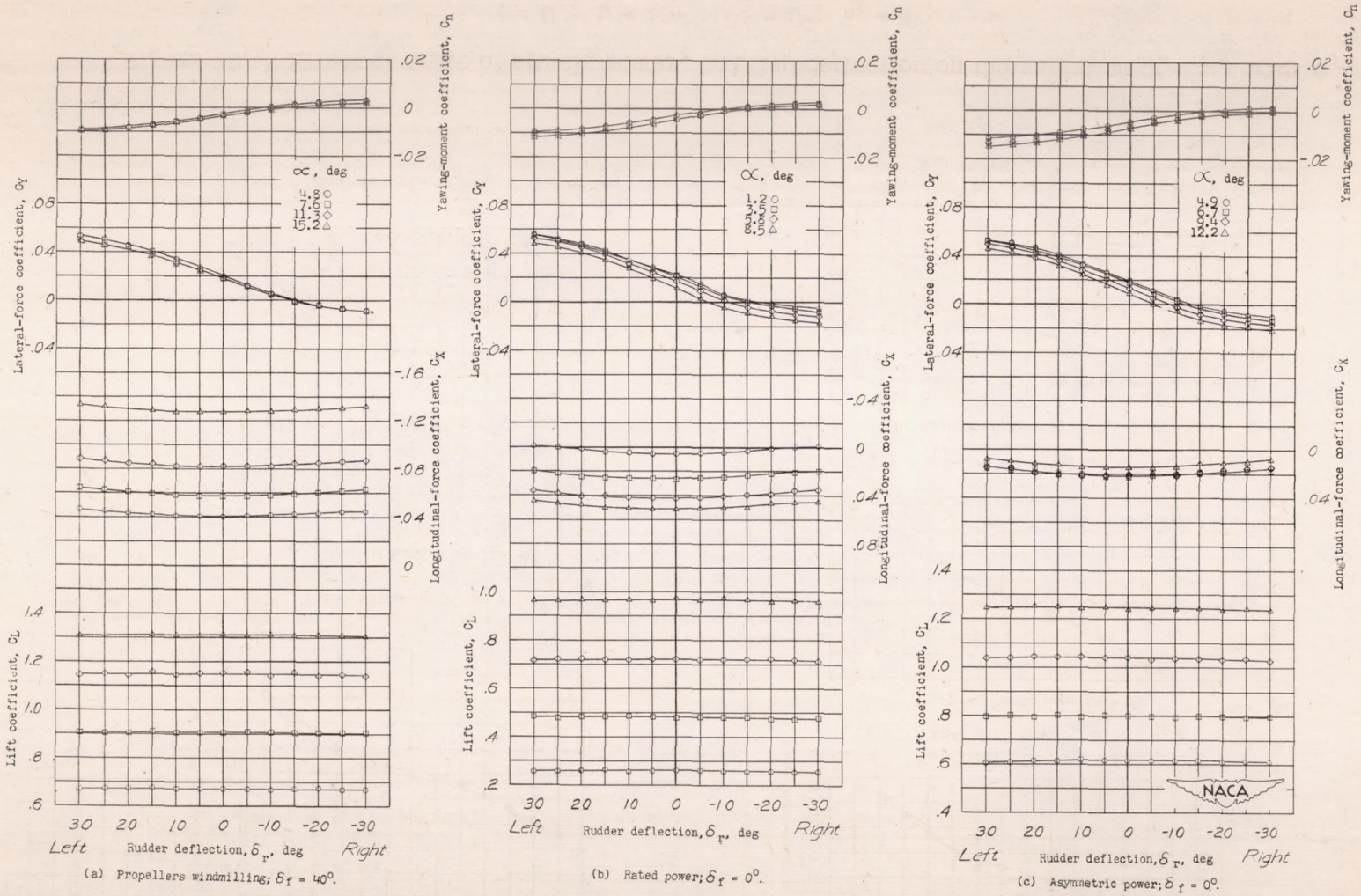

Figure 31.- Effect of angle of attack, power, and flap deflection on the variation of C_L, C_X, C_Y, and C_n with δ_r. $\psi = 5^\circ$; $i_t = 5.4^\circ$; $\delta_a = 0^\circ$; $\delta_e = 0^\circ$.

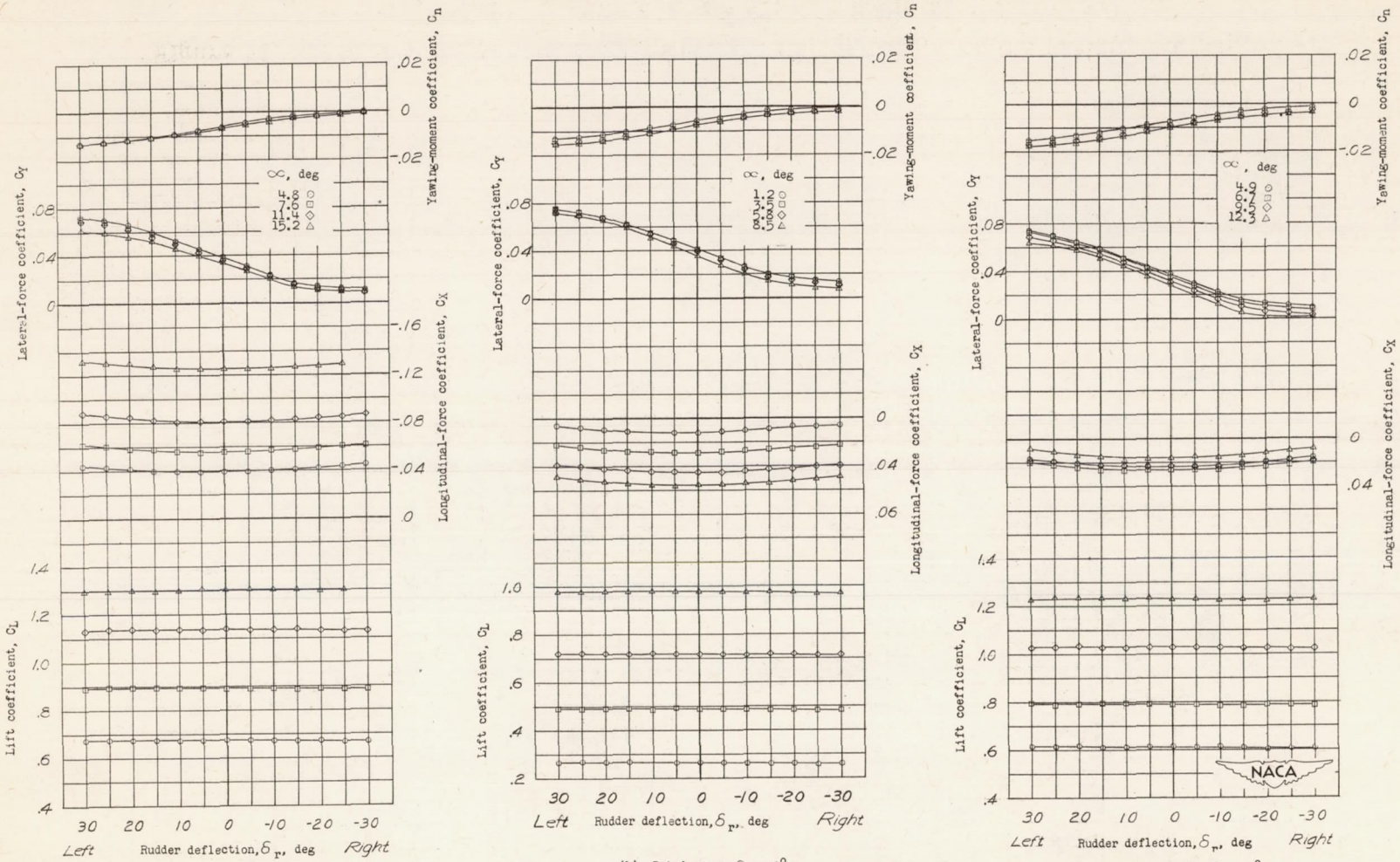

(a) Propellers windmilling; $\delta_f = 40^\circ$.

(b) Rated power; $\delta_f = 0^\circ$.

(c) Asymmetric power; $\delta_f = 0^\circ$.

Figure 32.- Effect of angle of attack, power, and flap deflection on the variation of C_L, C_X, C_Y, and C_n with δ_r. $\psi = 10^\circ$; $i_t = 5.4^\circ$; $\delta_a = 0^\circ$; $\delta_e = 0^\circ$.

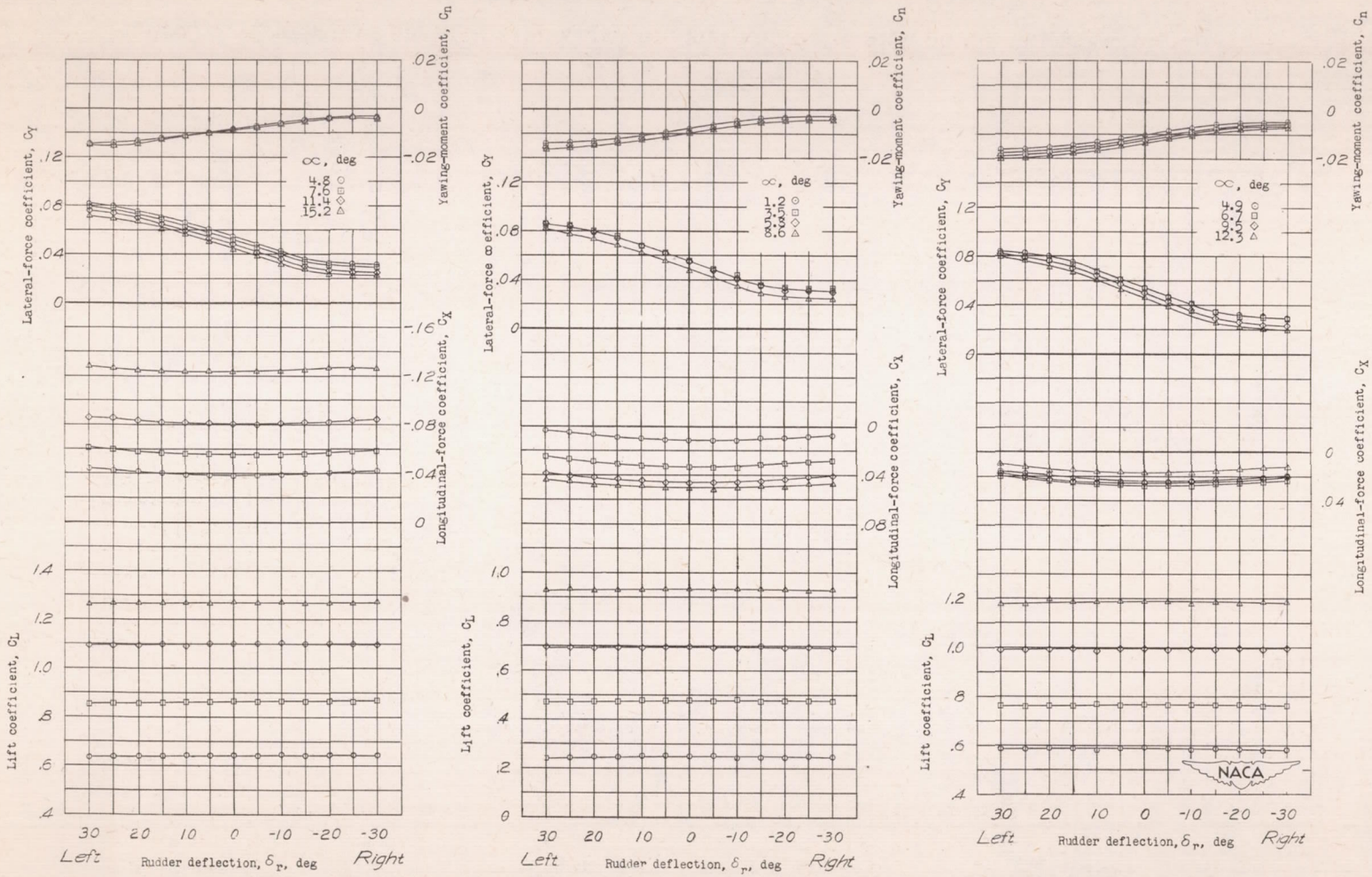

(a) Propellers windmilling; $\delta_f = 40^\circ$

(b) Rated power; $\delta_f = 0^\circ$.

(c) Asymmetric power; $\delta_f = 0^\circ$.

Figure 33.- Effect of angle of attack, power, and flap deflection on the variation of C_L, C_X, C_Y, and C_n with δ_r. $\psi = 15^\circ$; $i_t = 5.4^\circ$; $\delta_a = 0^\circ$; $\delta_e = 0^\circ$.

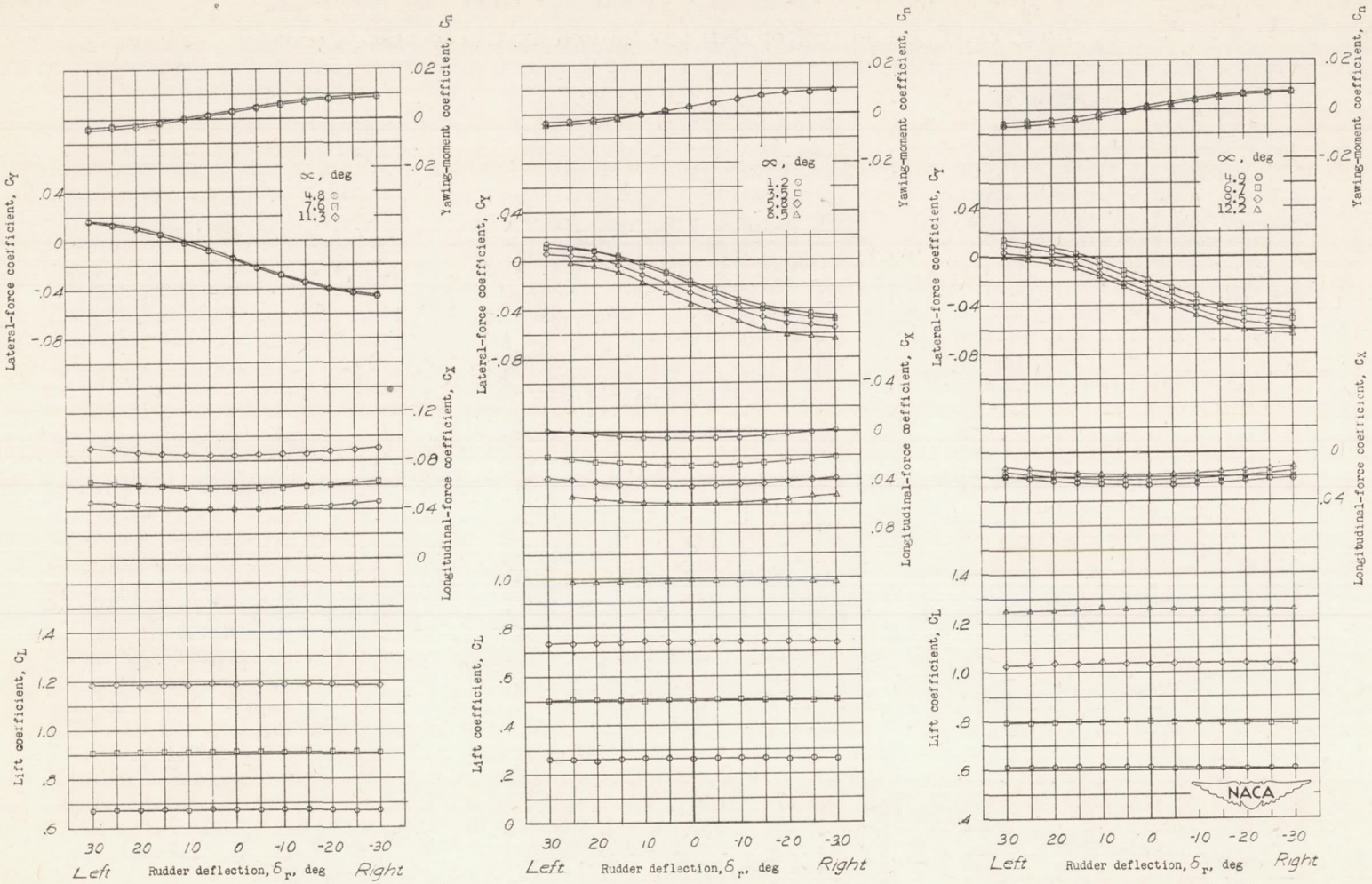

(a) Propellers windmilling; $\delta_f = 40^\circ$.

(b) Rated power; $\delta_f = 0^\circ$.

(c) Asymmetric power; $\delta_f = 0^\circ$.

Figure 34.- Effect of angle of attack, power, and flap deflection on the variation of C_L, C_X, C_Y, and C_n with δ_r. $\psi = -5^\circ$; $i_t = 5.4^\circ$; $\delta_a = 0^\circ$; $\delta_e = 0^\circ$.

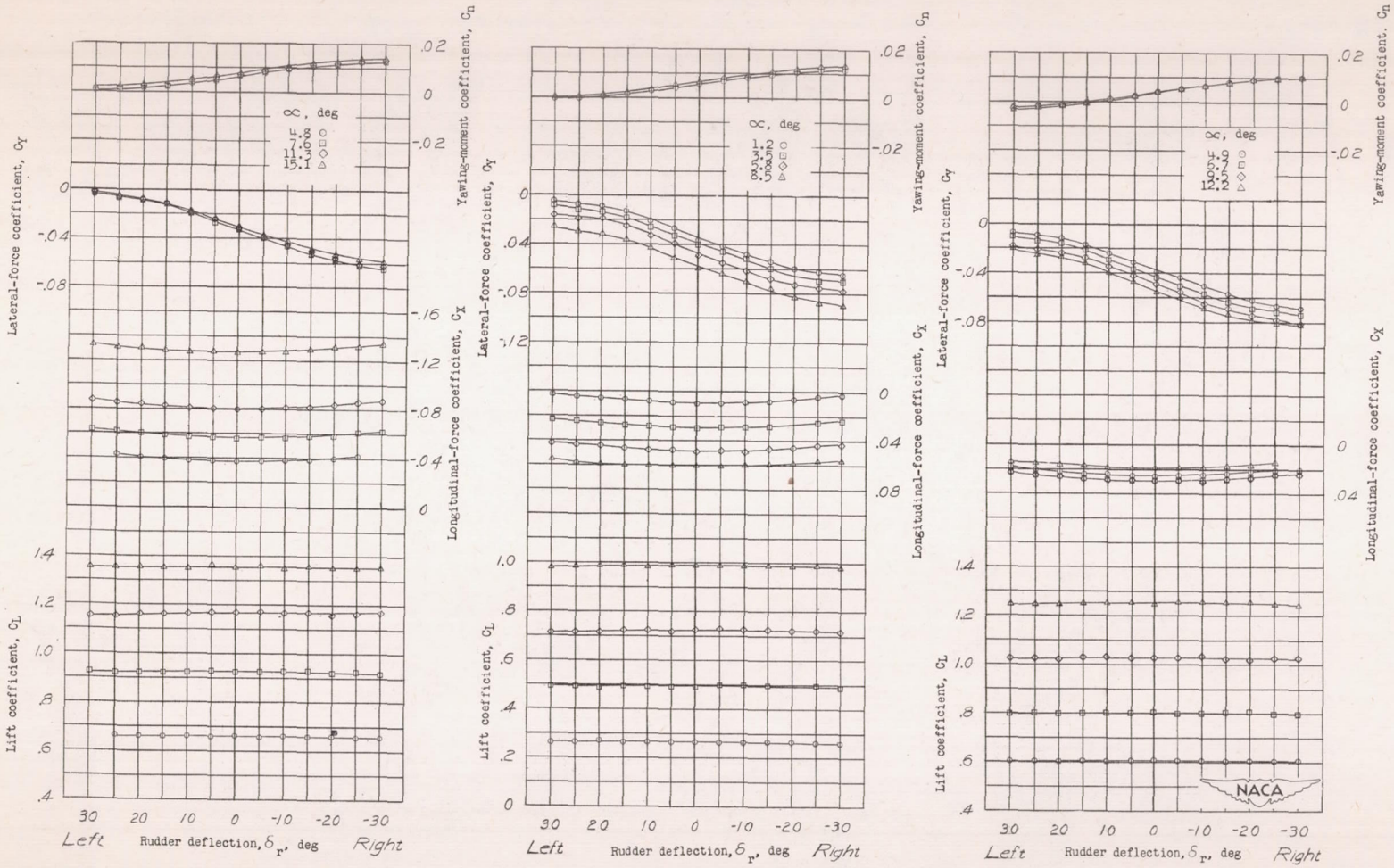

(a) Propellers windmilling; $\delta_f = 40^\circ$.

(b) Rated power; $\delta_f = 0^\circ$.

(c) Asymmetric power; $\delta_f = 0^\circ$.

Figure 35.- Effect of angle of attack, power, and flap deflection on the variation of C_L, C_X, C_Y, and C_n with δ_r. $\psi = -10^\circ$; $i_t = 5.4^\circ$; $\delta_a = 0^\circ$; $\delta_e = 0^\circ$.